Applied Geochemistry 191 (2025) 106529

Contents lists available at ScienceDirect

Applied Geochemistry

journal homepage: www.elsevier.com/locate/apgeochem

C-based gas (CH_4 and CO_2) fluxes from eutrophicated volcanic shallow lakes in Corvo Island (Azores, Portugal)

J. Virgílio Cruz [a,b,*], César Andrade [a], Duarte Toubarro [b,c], Letícia Ferreira [a], Adriano Pimentel [a], Fátima Viveiros [a,b], Franco Tassi [d,e], António Cordeiro [a], Diogo Braga [a], Pedro Raposeiro [f,g]

[a] IVAR – Instituto de Investigação em Vulcanologia e Avaliação de Riscos, Universidade dos Açores, Ponta Delgada, Portugal
[b] Faculdade de Ciências e Tecnologia, Universidade dos Açores, Ponta Delgada, Portugal
[c] CBA – Centro de Biotecnologia dos Açores, Universidade dos Açores, Ponta Delgada, Portugal
[d] Department of Earth Sciences, University of Florence, Florence, Italy
[e] Institute of Geosciences and Earth Resources, National Research Council of Italy, Italy
[f] CIBIO – Centro de Investigação em Biodiversidade e Recursos Genéticos & Laboratório Associado InBio, Portugal
[g] UNESCO Chair – Land Within Sea: Biodiversity & Sustainability in Atlantic Islands, Ponta Delgada, Portugal

ARTICLE INFO

Editorial handling by: Elisa Sacchi

Keywords:
CO_2 flux
CH_4 flux
Microbial communities
Microbial processes
Volcanic lakes
Azores

ABSTRACT

A study to investigate spatial and temporal variations on the diffusive CO_2 and CH_4 fluxes in two volcanic shallow lakes on Corvo Island (Azores) was made, coupling geochemical and microbial tools. Water in both lakes is from the Na–Cl type, depicting alkaline pH values and low EC (63–90 μS cm^{-1}). The total CO_2 flux (calculated using sequential Gaussian simulation) range between 2.5 t km^{-2} d^{-1} and 6.5 t km^{-2} d^{-1}, values closer to the mean value for lakes in the Azores with depth lower than 5 m. Values of total methane flux values are much lower, ranging from 31 to 38 kg km^{-2} d^{-1} falling in the lower range of worldwide datasets. Those emissions depict a seasonal effect, as total GHG emissions (CO_2 plus CH_4) range from 0.66 to 1.1 t $CO_{2\text{-eq}}$ d^{-1} in warmer conditions, about twice the values during colder periods.

The microbial characterization also depicts seasonal variations, showing a close relation with the diffusive CO_2 and CH_4 fluxes. During winter, anaerobic and sulfate-reducing bacteria are abundant, when microbial respiration intensifies, while in summer an enrichment in fermentative bacteria, including *Clostridiaceae* and *Enterobacteriaceae* is observed. High CH_4 production in summer results is expected from the presence of methanogenic archaea, instead methane oxidation is more relevant in winter, as shown by the higher abundance of methanotrophs, such as *Methylomonadaceae* and *Methylococcaceae*. Results show that small volcanic lakes are significative natural sources of C-based greenhouse gases, being CO_2 and CH_4 emissions enhanced by the trophic state of lake ecosystems.

1. Introduction

Rising carbon dioxide levels in the atmosphere have been observed in the last decades, resulting from emissions toward the atmosphere from major sources, such as combustion of fossil fuels, deforestation, agricultural practices, or the production of cement (Nunes, 2023). Surface water bodies have been also identified as important natural sources of C-based greenhouse gases, namely CO_2 and CH_4, and may therefore contribute to global warming. In lakes the major drivers that control greenhouse gases (GHG) emission are the size of the water body and their trophic state (Bhushana et al., 2024). Even if methane flux (ΦCH_4) from surface water bodies are lower than those of carbon dioxide flux (ΦCO_2), methane has global warming potential 27 times greater than carbon dioxide over a 100-year period (Forster et al., 2021), thus also contributing to the observed rise of the methane that doubled the pre-industrial values (Wuebles and Hayhoe, 2002) and experiences high increasing rates in the last years (Nisbet et al., 2019).

Despite some uncertainty, several estimations have been presented regarding global CO_2 emission from lakes, ranging from 2.44×10^2 to 1.4×10^3 Tg yr^{-1} (Cole et al., 1994; Tranvik et al., 2009; Raymond et al., 2013; Holgerson and Raymond, 2016; DelSontro et al., 2018).

Methane emissions from surface water bodies have received increasing worldwide attention in the last decades, since the early estimates provided by Ehhalt (1974), Smith and Lewis (1992), St. Louis

* Corresponding author. Rua Mãe de Deus, Edifício do Complexo Científico, 3° Andar - Ala Sul, Ponta Delgada, 9500-321, Açores, Portugal.
E-mail address: jose.vm.cruz@uac.pt (J.V. Cruz).

https://doi.org/10.1016/j.apgeochem.2025.106529
Received 27 February 2025; Received in revised form 7 August 2025; Accepted 11 August 2025
Available online 11 August 2025

et al. (2000) and Bastviken et al. (2004). Since this pioneering work, and despite the reported uncertainties, global estimates have been proposed for different types of surface water bodies such as lakes (e.g. Bastviken et al., 2011 and references therein), wetlands (Cao et al., 98; Walter et al., 2001; Zhu et al., 2015) and rivers (Rocher-Ros et al., 2023). Following wetlands, lakes represent the second-larger second aquatic source of CH_4 to atmosphere, and total methane emissions from these water bodies range 8–75 Tg yr^{-1} (Smith and Lewis, 1992; Bastviken et al., 2004, 2011; Saunois et al., 2016, 2020; Johnson et al., 2022). These methane emissions from lakes worldwide correspond to about 37.9 % of the inland waters and explain about 35 % of emissions from global aquatic environments (Rosentreter et al., 2021).

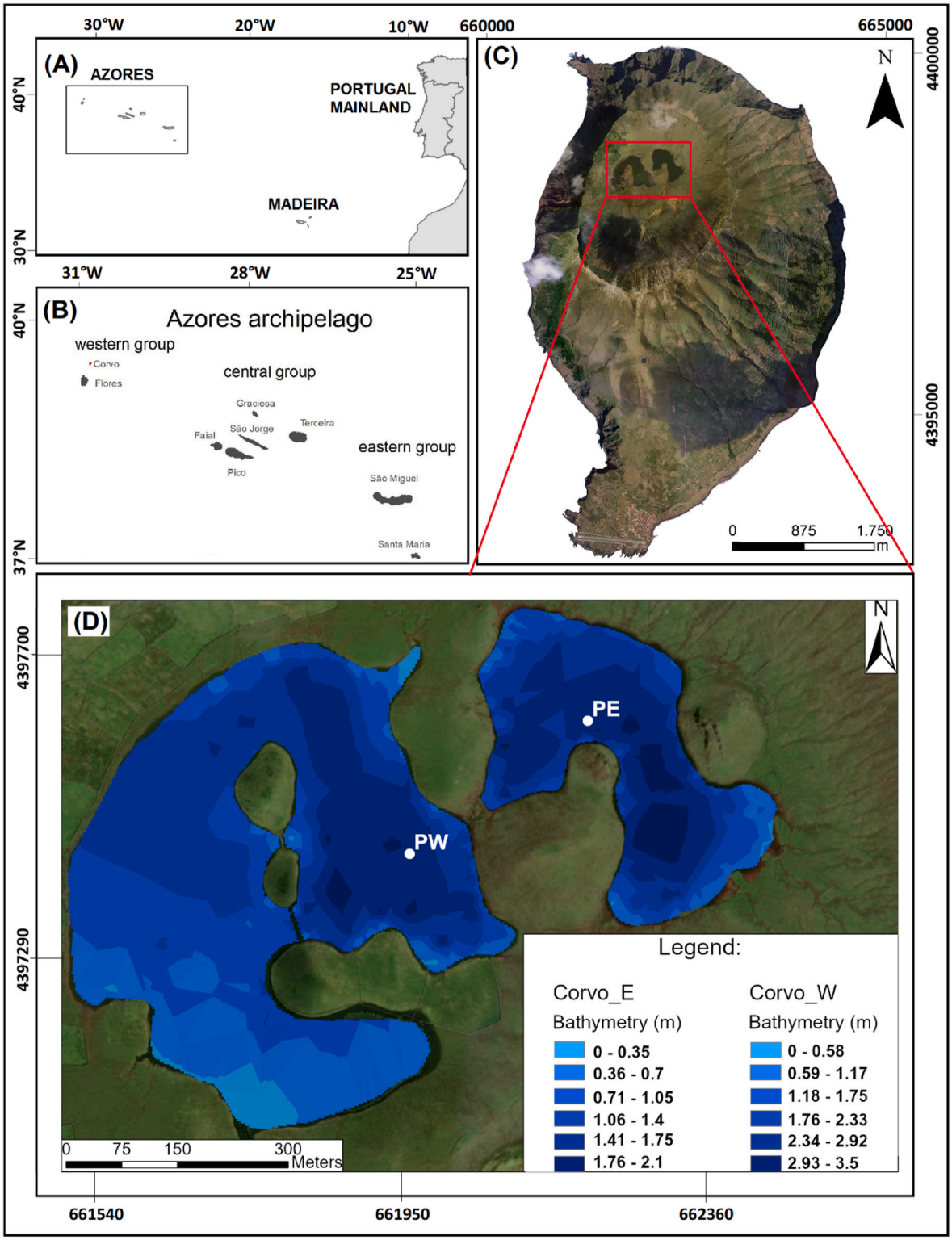

Fig. 1. – Location of the studied lakes in the Azores archipelago (Portugal). A, location of the Azores archipelago in the North Atlantic Ocean; B, location of the Corvo Island (in red) in the Azores; C, the island of Corvo with the studied area outlined in red; D, Caldeirão W (left) and Caldeirão E (right) lakes in the floor of the summit caldera of the Caldeirão central volcano (UTM coordinates are used for plots C and D; UTM zone 25 N).

Despite all studies made so far, further research is needed to estimate methane emission from lakes at diverse spatial and temporal scales, allowing also to a better knowledge of the several drivers that control fluxes across lakes surface, such as salinity (Liu et al., 2024), depth (Li et al., 2021), temperature (Duc et al., 2010), water level (Yuan et al., 2021). Most of these drivers are reflected in data seasonality already characterized in various studies (Lesley and Lewis, 1992; Eugster et al., 2020). Moreover, methane emissions are also influenced by the trophic state of the lake ecosystems, with higher emissions often associated with eutrophic conditions (e.g. Beaulieu et al., 2019).

The Azores archipelago consists of nine volcanic islands, located in the North Atlantic Ocean between latitudes 37°N and 40°N and longitudes 25° and 31°W, approximately 1500 km off the coast of mainland Portugal, covering a total area of 2322 km^2 (Fig. 1A). Corvo island is the smallest of the archipelago, with an area of 17.1 km^2 and about 27 inhabitants per km^2 (Fig. 1B). The studied lakes – the so-called Caldeirão West (W) and Caldeirão East (E) lakes – are in the summit caldera of the central volcano with the same name that dominates the geology of Corvo Island (Fig. 1C to D; Fig. S1 – supplementary material).

Due to the significant number of lakes in the Azores, and their respective importance as strategic water resources and for tourism, eutrophication has been a subject of study for several decades (Porteiro, 2000; Santos et al., 2005; Ribeiro et al., 2008; Martins et al., 2008, 2012; Gonçalves, 2008; Pacheco et al., 2005, 2010; Cruz et al., 2015; Malcata et al., 2022). Moreover, numerous studies have examined changes in lake water chemistry in relation to volcanic activity (Martini et al., 1994; Cruz et al., 2006; Andrade et al., 2024). Based on research conducted over the past decade (Andrade et al., 2016, 2019a, 2019b, 2019c, 2019d, 2020a, 2020b), CO_2 emission from the surface of 45 lakes in the Azores were estimated to be approximately 171×10^3 t yr^{-1}, with 42 % of these emissions originating from volcanic activity ($\sim 72 \times 10^3$ t yr^{-1}; Andrade et al., 2021). In contrast, methane emissions from Azorean lakes remain largely unstudied. The only work to address this subject so far is by Tassi et al. (2018), who investigated the mechanisms controlling CH_4 release from five lakes on São Miguel Island.

Building on the possible contribution of GHG emissions from small lakes, that may be enhanced by the active volcanic setting of some water bodies, a study was made to test the importance of this process. Moreover, water bodies in small oceanic lakes have been somehow neglected in emissions inventories made so far, and in archipelagos such the Azores a high number of similar water bodies may occur. Therefore, the present research aimed to characterize the diffusive ΦCO_2 and ΦCH_4 in two lakes located on Corvo, the westernmost island of the Azores archipelago (Fig. 1A and B), in a spatial and temporal perspective, and identify the main drivers that control the emissions of these important GHGs, with a particular focus on eutrophication.

2. Methodology

2.1. Geological setting

Corvo Island is a small volcanic edifice with an overall N–S elongation, some 6 km in length and 4 km in width. The morphology of the island is dominated by a central volcano (maximum altitude of 720 m a.s.l.), characterized by strongly asymmetric flanks and a roughly elliptical caldera (known as Caldeirão), with 2.3 by 1.8 km across and a depth of about 300 m. The western and northern slopes of the island are deeply eroded, forming steep coastal cliffs up to 500–700 m high. In contrast, the eastern and southern slopes have smoother morphologies, lower cliffs (up to 200 m high) and a few scoria cones. The row of large horseshoe-shaped scoria cones on the southern slope and the coastal lava delta that forms the southern tip of the island constitute the other main geomorphological unit of the volcanic edifice (Dias, 2001; França et al., 2003; Pacheco et al., 2013; Melo et al., 2018).

The volcanostratigraphy of Corvo is organised into three main units that reflect different phases of the geological history of the island (França et al., 2003): a Pre-caldera unit, that includes all products related to the initial volcanism of Corvo (estimated age around 1.5–1.0 M yr), a Syn-caldera unit, that comprises pumice fall deposits, surges, pyroclastic flow deposits (of trachyandesitic to phonolitic composition), and lahars, and a post-caldera unit, that includes the most recent basaltic lavas (estimated age around 80–100 k yr) (França et al., 2003; Larrea et al., 2013). Both Caldeirão lake fills in the depressions between scoria and spatter cones lying on the caldera floor, which are part of the post-caldera stratigraphic unit. The impermeabilization of the bottom of the caldera may have resulted from the deposition of ash and scoria lapilli associated with the eruption of the cones. Although the ages of the cones and pyroclastic deposits are unknown, the earliest lake sediments that cover these volcanic deposits are dated at approximately 4.2 k yr cal BP (Sáez et al., 2025).

2.2. Hydrological setting

The average annual precipitation on Corvo island is estimated as 1144.6 mm yr^{-1}, that despite being lower than the mean value for the archipelago is higher than the mean actual evapotranspiration (736 mm yr^{-1}) (DROTRH, 2001). Nevertheless, at altitude the average annual precipitation may reach values as high as 2400 mm yr^{-1}, which coupled with the expected mean annual temperature in these areas (~12 °C) relative to the value observed near the sea (17.5 °C), thus influencing evapotranspiration, should increase surface runoff.

The main characteristics of both Caldeirão lakes are summarized in Table S1 (supplementary material). Caldeirão W and Caldeirão E are two lakes closely located at approximately 390 m above sea level, lying on the caldera floor of the Caldeirão volcano, being the surface area and maximum depth of the former respectively equal to 0.19 km^2 and 3.4 m (Fig. 1D). Instead, Caldeirão E Lake presents a lower surface area and depth, respectively equal to 0.07 km^2 and 2.0 m. The respective storage volumes are relatively small, equal to 1.6×10^4 and 9.2×10^4 m^3, respectively.

From the overall runoff inflow to both lakes, estimated as 2.9×10^6 m^3 yr^{-1} (DROTRH, 2021), and considering the storage volume of both lakes, it's possible to compute a residence time of 8.79×10^{-2} yr for the lakes. The only source of uncertainty in the residence time computation is associated to the runoff to the lakes, as direct rainfall input is negligible, due to the relatively small surface area of both lakes, and spring discharges or artificial inflows along the lake margins do not occur. Moreover, groundwater seepage is unlikely to occur due to the altitude and the expected groundwater flow paths in the island.

Both lakes are considered to be in moderate ecological status following Water Framework Directive (WFD) criteria due to ongoing eutrophication (DROTRH, 2021). This status is associated with land use inside the volcanic caldera, where pastureland (10.8 %) is to be observed, being the nutrient load to the lake calculated as 0.64 t yr^{-1} and 0.08 t yr^{-1}, respectively for nitrogen and phosphorus (DROTRH, 2021).

2.3. Water chemistry methodology

Lake water composition in the two Caldeirão lakes was assessed over four surveys conducted across four distinct periods: late spring (1st survey – May 2023), summer (2nd survey – August 2023), late autumn (3rd survey – November 2023) and winter (4th – January 2024). These surveys were planned to capture seasonal variability, despite the continuous mixing conditions along the water column all through the year. A 1L SEBA sampling bottle was used for the collection of water samples. The collection on Caldeirão W Lake took place at 1-m depth interval, totalizing 14 samples, while on Caldeirão E Lake, due to the lower depth, samples were collected at the surface, at the middle and at the bottom of the water column, totalizing 12 samples (locations PW and PE, respectively for Caldeirão W and Caldeirão E lakes; Fig. 1D).

Physico-chemical parameters, including pH, temperature, and

electrical conductivity (EC), were measured immediately after sampling using a portable multi-parameter meter (WTW Multi 3620 IDS), and alkalinity and dissolved carbon dioxide concentrations were determined in the field by titration following APHA-AWWA-WPCF (1985) guidelines. Despite the uncertainties associated with the latter titrations, dissolved CO_2 values allow us to evaluate the differences along the water column. The sampling and analytical procedures were fully described by Andrade et al. (2016).

Along the 1st survey, two additional samples were collected from both lakes at the surface and bottom of the water column for the $^{13}C/^{12}C$ stable isotopic ratio analysis. Sampling procedures for DIC $\delta^{13}C$ samples followed the International Atomic Energy Agency guidelines (IAEA, 2017). These samples were analyzed at the Stable Isotope Laboratory of Estación Biológica Doñana (CSIC) using a continuous-flow isotope-ratio mass spectrometry system (Thermo Electron), interfaced with a Flash HT plus elemental analyzer and a Delta V Advantage mass spectrometer. The maximum error interval for $\delta^{13}C$ was ±0.15 ‰.

2.4. CO_2 flux methodology

ΦCO_2 measurements were performed using portable equipment, following the accumulation chamber method (Chiodini et al., 1998), with adaptations to account for the equipment floatability (Mazot and Bernard, 2015). This technique has been widely used (e.g. Mazot and Taran, 2009; Hernández et al., 2011), and the equipment and procedures description was comprehensively described in other studies made in the Azores (Andrade et al., 2016, 2019a, 2021).

ΦCO_2 were taken at the surface of each lake on the same days water samples were collected, resulting in 176 and 189 measurements at Caldeirão W Lake for the 1st and 2nd surveys, respectively, and 146 and 113 measurements at Caldeirão E Lake. The measurement network spanned approximately 0.18 km^2 for Caldeirão W and 0,07 km^2 for Caldeirão E, following a uniform grid as possible. Measurements were performed at each node in the network by deploying the chamber at the lake surface. Each measurement took just enough time to assure the increase of CO_2 inside the chamber during a certain period, usually 60 s (but sometimes as high as 2 min), after which the boat moved quickly rowing to the next point, which took a few seconds. The small area of each lake allowed measurements to be taken in each lake in a limited time frame, which reduces the potential error of comparing data obtained at different times of the day. The GPS coordinate of each measurement was recorded, alongside water depth measurements obtained using a Garmin ECHOTM 500c bathymetric probe. Wind velocity was measured at a 5 min-interval all along field surveys, using a portable equipment (weather center by PCE instruments - reference PCE FWS 20 N).

Two statistical methods were applied to the ΦCO_2 data: the Graphical Statistical Approach (GSA) (e.g. Chiodini et al., 1998) and the sequential Gaussian simulation (sGs) (Cardellini et al., 2003). GSA is based on cumulative probability plots, which aid in identifying distinct populations within the dataset (Sinclair, 1974), while sGs involves multiple simulations of spatial distribution of the attribute (e.g. ΦCO_2 in the lake) to generate final degassing maps. The sGs method enables us to preserve the spatial variability of the measured attributes as, contrary to kriging techniques, doesn't smooth extreme values, producing realizations that follows the original data structure (Isaaks and Srivastava, 1989; Deutsch and Journel, 1998). A detailed discussion on the rational and procedures associated with each statistical method can be found in Andrade et al. (2016 and references therein).

The E-type probability maps are subsequently visualized using ArcGIS software vs. 10 (ESRI). The total diffuse ΦCO_2 was estimated by integrating the mean values derived from the sGs over the total area of the lake. This methodology is commonly used in studies of CO_2 emissions in volcanic regions worldwide (e.g. Cardellini et al., 2003; Hernández et al., 2011; Mazot and Bernard, 2015), and in studies conducted in the Azores (Viveiros et al., 2010; Andrade et al., 2016, 2021).

2.5. Methane flux methodology

2.5.1. Empirical measurement of ΦCH_4

Static floating chambers (SFC) were used along multiple transects in Caldeirão lakes to proceed to the collection of gas samples, allowing the determination of the ΦCH_4 from the earth surface to the atmosphere. This approach is an adaptation of the static gas chamber method commonly used for measuring gaseous diffuse fluxes from soils (Livingston and Hutchinson, 1995 and references therein). Samples were taken considering the increase of CH_4 concentration over time within a chamber of known geometry (Cole et al., 2010). Therefore, samples were collected at each SFC at two different time intervals, 3 min after placing the chamber in the water and again after 30 min. In lakes, near-surface turbulence controls gas transfer velocity, being mainly driven by atmospheric forcing (Guseva et al., 2021). Nevertheless, field surveys were conducted in steady environmental conditions to avoid potential disturbances deriving from environmental factors, such as the wind speed or wind-derived surface waves, thus limiting turbulence. Moreover, to prevent the SFCs from drifting, the latter were tied to a guide rope, which connected one side of the lake to the other.

The ΦCH_4 measurements were taken during the 3rd and the 4th surveys. Each transect consisted of six SFC placed at regular intervals along a straight line. At each of the Caldeirão lakes 2 transects (12 SFC measurements) were made in the 3rd survey and 6 transects (36 SFC), in the 4th. Transect locations were carefully selected to ensure representativeness, guided in part by the results over the early samples collected along the 3rd survey which allowed to enlarge the sampling network in the following 4th survey. In addition to gas samples, water temperature, pH, dissolved O_2, the depth of the water column and air temperature were measured at each SFC location. Wind velocity was also measured along 5 min-intervals, using the same equipment as for CO_2 flux.

Each SFC was constructed from the lower part of a HDPE bucket, which was cut to create containers with a diameter of 40 cm and a height of 14 cm. To assure floatability an inflated inner tube from a tire was used, to which the container was well fitted to prevent air from entering. When placed in water, approximately 2–3 cm of the tire submerged, sealing the inner chamber from the atmosphere. At the top of the container a small opening was fitted with a three-way valve, which was used to collect samples and remained closed until sampling extraction, to which a syringe was connected. Samples were taken to a vial, which was previously filled with slightly acidified (pH ~4) deionized water to avoid CO_2 dissolution, that was expelled as the sample was injected using a two-needle system.

Following sample collection, the gas analysis was conducted using gas chromatography at the Department of Earth Sciences, University of Florence (Italy). A Shimadzu 14A system equipped with a flame ionization detector and a 10-m long stainless-steel column packed with Chromosorb PAW 80/100 mesh was used for the analysis.

ΦCH_4 in each SFC was estimated using a mathematical expression from Tassi et al. (2013), that considers the increment of the methane concentration inside the chamber over time and their ratio between the volume and the basal area.

2.5.2. Theoretical computation of ΦCH_4

Dissolved gas samples were collected at each SFC location by filling a 30-mL glass vial beneath the lake surface, to avoid gas bubbles inside. He was injected into vials to allow headspace to dissolved gases equilibration. These samples were subsequently analyzed for the determination of dissolved gases concentration (CO_2, N_2, Ar, CH_4, O_2) using gas chromatography at the Department of Earth Sciences, University of Florence (Italy), using the same equipment as for the gas samples taken with the SFC with a 5-m-long stainless-steel column packed with Chromosorb PAW 80/100 mesh and coupled to a thermal conductivity detector.

To estimate the diffusive ΦCH_4 across the water-air interface, the thin boundary layer model (TBL; Liss and Slater, 1974). The required gas

transfer velocity was calculated from a value previously normalized to a Schmidt number of 600, following Crusius and Wanninnkhof (2003). For that purpose, wind speed data was considered, and the Schmidt number was calculated as function of temperature through a fourth order polynomial (Wanninnkhof, 2014). A full explanation of the calculation procedure, that includes the equations required, was published by Venturi et al. (2021). Whenever needed, correlation coefficients between some variables were computed using data analysis tools from Ms Excel.

2.6. Microbial communities and DNA extraction methodologies

Sediment samples were collected during summer (2nd survey) and winter (4th survey) from locations PW and PE, situated at Caldeirão W and Caldeirão E lakes (Fig. 1D) using a gravity sediment corer that was driven into the bottom sediments to a depth of 20–40 cm. From each 10 cm-internal diameter core, the top 1–2 cm was discarded, and the next 5 cm were kept into sterile plastic bags. During transportation, bags were kept chilled and protected from ambient light, and after reachin laboratory were preserved at −80 °C until analysis. DNA extraction was performed on 250 mg of sediment using the DNeasy PowerSoil Pro Kit (QIAGEN). For each homogenized core, DNA from three pooled subsamples was quantified using the Qubit™ dsDNA HS/BR Assay Kits (Invitrogen).

Full-length 16S rRNA gene sequencing was conducted using the PacBio SMRT third-generation sequencing platform. The variable regions V1–V9 of the 16S rRNA gene were amplified using the universal primer set 27F (AGRGTTYGATYMTGGCTCAG) (Stackebrandt and Goodfellow, 1991) and 1492R (RGYTACCTTGTTACGACTT), with a specific PacBio barcode assigned to each sample. Amplicons were carried out using the KAPA SYBR FAST qPCR Kit, pooled into equimolar concentrations. The pooled amplicons were processed with the SMRTbell Express Template Prep Kit 2.0 (PacBio, USA) following the protocol. Sequencing was completed on the Sequel II PacBio system using the Sequel II Sequencing Kit 2.0.

Raw sequencing reads underwent quality filtering to remove low-quality sequences and chimeras through the MOTHUR pipeline. High-quality reads were grouped into operational taxonomic units (OTUs) and assigned taxonomically by alignment to the SILVA 138 database.

Microbial community composition was compared between Caldeirão W and Caldeirão E lakes and between seasonal periods using a range of statistical analyses. Alpha diversity was evaluated using species richness and Shannon diversity indices. Beta diversity was analyzed through principal coordinate analysis (PCoA) based on Bray-Curtis dissimilarity matrices. Significant differences in community compositions were evaluated with permutational multivariate analysis of variance (PERMANOVA). Differential abundance testing was conducted to detect taxa exhibiting significant seasonal or spatial variations. All statistical analyses were performed in R using the 'vegan' and 'DESeq2' packages.

3. Results

3.1. Water composition

Descriptive statistics for the physico-chemical parameters and major-ion concentrations in the samples collected from both lakes are presented in Table S2 (supplementary material). Water temperatures at Caldeirão W Lake ranged from 12.2 °C to 26.6 °C (mean = 17.8 ± 4.7 °C), while at Caldeirão E temperatures varied from 12.8 °C to 27.5 °C (mean = 19.0 ± 5.6 °C). Both water bodies are in full mixing conditions throughout the year, being the highest temperature difference between the surface and the bottom equal to 2.6 °C (Caldeirão W) (Fig. S2–A – supplementary material). The highest water temperatures were observed during the 2nd survey, with values in the range of 26.9 °C to 27.5 °C, and between 23.9 °C to 26.6 °C at Caldeirão E and Caldeirão W, respectively, and the lowest values, as high as 13.2 °C, were the ones measured during the 4th survey.

The pH values tend to be slightly lower at Caldeirão E comparing to Caldeirão W, ranging in the former from 6.80 to 8.20 (mean = 7.54 ± 0.46) and at the latter from 7.09 to 8.67 (mean = 7.86 ± 0.46), with minor variations being observed along the water column (Fig. S2–B – supplementary material). Dissolved CO_2 is slightly higher in Caldeirão E Lake, being in the range between 1.5 and 2.6 mg L^{-1} (mean = 2.0 ± 0.4 mg L^{-1}), compared to values in Caldeirão W, that ranged between 1.4 and 2.1 mg L^{-1} (mean = 1.8 ± 0.2 mg L^{-1}). The major gradients along the water column are observed at Caldeirão E (Fig. S2–D – supplementary material).

Electrical conductivity (EC) tends to be slightly higher in Caldeirão E Lake relative to Caldeirão W. In the former, EC ranged between 64 and 89 µS cm^{-1} (mean = 74 ± 10 µS cm^{-1}), while in the latter values ranged between 63 and 90 µS cm^{-1} (mean = 77 ± 9 µS cm^{-1}). In both lakes the highest values were observed during the 1st survey, reaching values as high as 90 µS cm^{-1} (Fig. S2–C – supplementary material).

Water types were primarily classified as Na–Cl (Fig. 2), reflecting that in both lakes chloride and sodium dominates the ionic content, with values in the range of 35.64 %–44.53 % and 26.05 %–40.36 % of the overall amount, respectively, reflecting the influence of sea salts deposition, one of the main drivers of lake water chemistry in the Azores (Cruz et al., 2006; Andrade et al., 2024).

The dissolved gas content at the surface of the analyzed lakes is largely dominated by N_2, comprising between 50.7 % and 61.2 % in Caldeirão W and between 53.8 % and 62.1 % in Caldeirão E Lake (Fig. S3 – supplementary material; Table S3 – supplementary material).

The N_2/Ar ratio varies from 38.1 to 43.6 and between 38.1 and 43.6, respectively at Caldeirão W and E, both values falling in the typical range of Air Saturated water (ASW), which range between 38 and 42. Carbon dioxide abundance ranges between ranges from 6.4 % to 12.3 % at Caldeirão W Lake, being similar at Caldeirão E, ranging from 6.4 % to 12.5 %. Methane levels remain below 1.1 %, with a noticeable decrease during the 4th survey. The N_2/O_2 molal ratio fluctuates between 2.45 and 4.50 during the 3rd survey, and between 2.50 and 3.10 in the 4th survey. At Caldeirão E, this ratio his even higher during the 3rd survey, being in the range of 2.60–5.30, while during the 4th survey aligns closely with values observed at Caldeirão W, ranging from 2.52 to 3.

3.2. ΦCO_2 measurements

ΦCO_2 measurements at Caldeirão W during the 1st survey range between 1.2 and 6.4 g m^{-2} d^{-1} (mean = 3.0 ± 1.0 g m^{-2} d^{-1}; median = 2.9 g m^{-2} d^{-1}), while during the 2nd survey the values ranged from 1.6 to 13.3 g m^{-2} d^{-1} (mean = 4.5 ± 2.1 g m^{-2} d^{-1}; median = 3.9 g m^{-2} d^{-1}) (Table 1). For Caldeirão E Lake, the ΦCO_2 values ranged from 0.3 to 6.3 g m^{-2} d^{-1} (mean = 2.1 ± 1.0 g m^{-2} d^{-1}; median = 2.1 g m^{-2} d^{-1}) and from 0.9 to 16.8 g m^{-2} d^{-1} (mean = 5.3 ± 3.4 g m^{-2} d^{-1}; median = 4.3 g m^{-2} d^{-1}), respectively (Table 1). In both cases, higher ΦCO_2 values were consistently higher during the 2nd survey compared to the 1st survey (Fig. 3A–B), especially in Caldeirão E Lake.

The cumulative probability plots further highlight that in most surveys just one population emerges, corresponding to measurements below the threshold of 35 g m^{-2} d^{-1}, that corresponds to the uppermost value beyond which a contribution from a deep-seated CO_2 source contributes to gaseous emissions (Andrade et al., 2016). During the 1st survey at Caldeirão E Lake, two distinct populations were identified, although they pointed to also to a single CO_2 source, with the first population (A) corresponding to very low ΦCO_2, ranging from 0.3 to 1.5 g m^{-2} d^{-1} and the second population (B) corresponding to slightly higher ΦCO_2 (1.6–6.3 g m^{-2} d^{-1}) (Fig. S4 – supplementary material).

Modeled variograms for ΦCO_2 data indicated a spherical or an exponential spatial structure, with nugget values ranging from 0.3 to 0.7 and 0.1 to 0.51 for Caldeirão W and Caldeirão E lakes (Figure S5-A to S5-D – supplementary material). The influence range of each measurement point relative to its neighboring values was between 90 and 120 m for

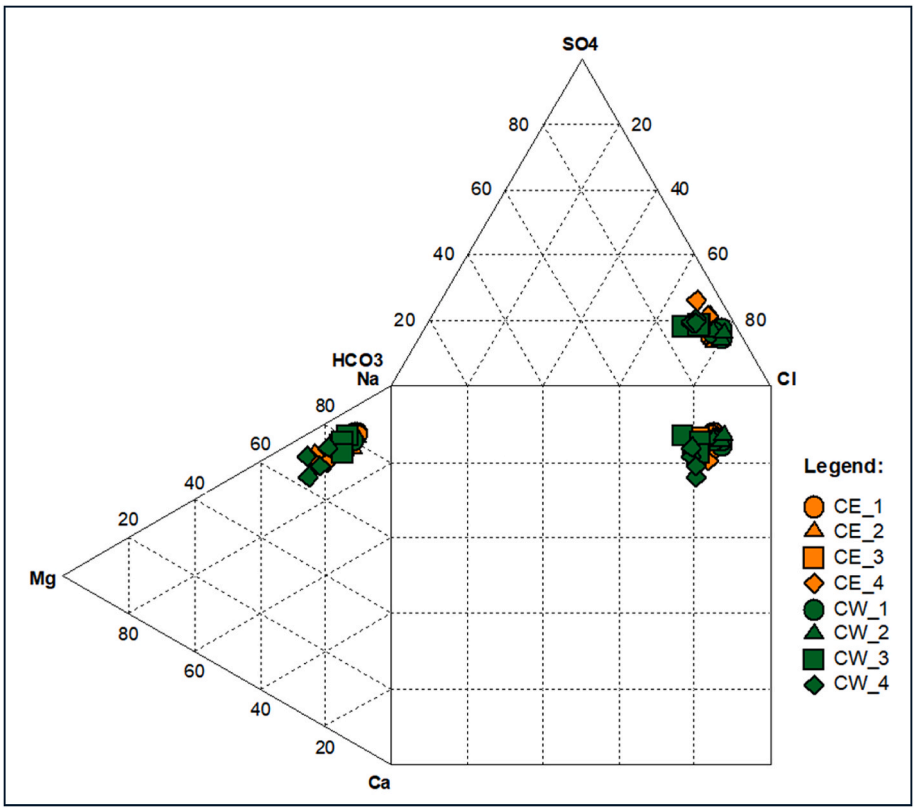

Fig. 2. – Durov-type diagram illustrating the relative major-ion composition of the water samples from the studied lakes.

Table 1
Descriptive statistics of ΦCO_2 in the Caldeirão lakes (W and E) presented according to the measurement survey (n, number of measurements).

Lake	Survey	n	Min. (g m^{-2} d^{-1})	Max. (g m^{-2} d^{-1})	Mean ± SD (g m^{-2} d^{-1})	Median (g m^{-2} d^{-1})
Caldeirão W	1	176	1.2	6.4	3.0 ± 1.0	2.9
	2	189	1.6	13.3	4.5 ± 2.1	3.9
Caldeirão E	1	146	0.3	6.3	2.1 ± 1.0	2.1
	2	113	0.9	16.8	5.3 ± 3.4	4.3

Caldeirão W (Figure S5-C and S5-D – supplementary material) and between 40 and 65 m for Caldeirão E (Figure S5-A and S5-B – supplementary material).

The spatial distribution of ΦCO_2 data shown by the mean CO_2 flux maps, generated for each lake by 100-equiprobable sequential gaussian simulations (Fig. 4A–B), depicts a homogeneous distribution of values across both lakes surface, except for an area in the upper north section of Caldeirão E lake during the 2nd survey (Fig. 4B).

3.3. ΦCH_4 measurements

The measured and calculated ΦCH_4 values across various transects for both surveys are presented by means of a boxplot in Fig. S6 (supplementary material). The datasets are also shown in Tables S4 and S5 (supplementary material), respectively for Caldeirão E and Caldeirão W lakes The theoretical estimates obtained using the TBL model closely match the field measurements, confirming the effectiveness of the survey methodology. This result is consistent with findings by Ghioldi (2021), who employed a similar field approach using SFC, and further compared field ΦCH_4 with values predicted by three different models, concluding that the most accurate theoretical approximation was achieved using the k_{600,CH_4} expression proposed by Crusius and Wanninnkhof (2003).

Measured ΦCH_4 at Caldeirão W Lake during the two surveys range from 0.034 to 0.042 g m^{-2} d^{-1} (mean = 0.038 ± 0.002 g m^{-2} d^{-1}; median = 0.038 g m^{-2} d^{-1}) for the 3rd survey, and from 0.017 to 0.051 g m^{-2} d^{-1} (mean = 0.031 ± 0.008 g m^{-2} d^{-1}; median = 0.029 g m^{-2} d^{-1}) for the 4th survey (Table 2). The interquartile range (IQR) was lower in the 3rd survey (0.002 g m^{-2} d^{-1}) compared to the 4th survey (0.011 g m^{-2} d^{-1}) indicating greater data variability in the latter survey. This variability is also shown by the spatial distribution of ΦCH_4 across both lakes, showing some heterogeneity along the 4th survey (Fig. 5A–B).

For Caldeirão E, the measured ΦCH_4 ranged from 0.031 to 0.039 g m^{-2} d^{-1} (mean = 0.043 ± 0.003 g m^{-2} d^{-1}; median = 0.035 g m^{-2} d^{-1}), in the 3rd survey, and from 0.008 to 0.033 g m^{-2} d^{-1} (mean = 0.022 ± 0.007 g m^{-2} d^{-1}; median = 0.024 g m^{-2} d^{-1}) in the 4th survey (Table 2). Like Caldeirão W, the IQR was slightly lower for the 3rd survey (0.003 g m^{-2} d^{-1}) relative to the 4th survey (0.007 g m^{-2} d^{-1}), reflecting greater dispersion in the latter.

3.4. Microbial communities

Overall, summer samples exhibited higher microbial richness and diversity, with Chao1 index values reaching 4770.63 in Caldeirão E and 4604.93 in Caldeirão W, compared to lower values in winter (Caldeirão E: 3855.6; Caldeirão W: 3299.4). The Shannon diversity index showed similar trends, with higher values in summer (Caldeirão E: 5.87; Caldeirão W: 5.30) than in winter (Caldeirão E: 4.19; Caldeirão W: 3.60), indicating a more complex and even microbial community during the warmer season (Table S6 – supplementary material). Rarefaction curve analysis confirmed that sequencing depth was sufficient to capture the microbial diversity within all samples, as the curves approached saturation (Fig. S7 – supplementary material).

Non-metric multidimensional scaling (NMDS) depicts clear clustering patterns, further highlighting differences between microbial

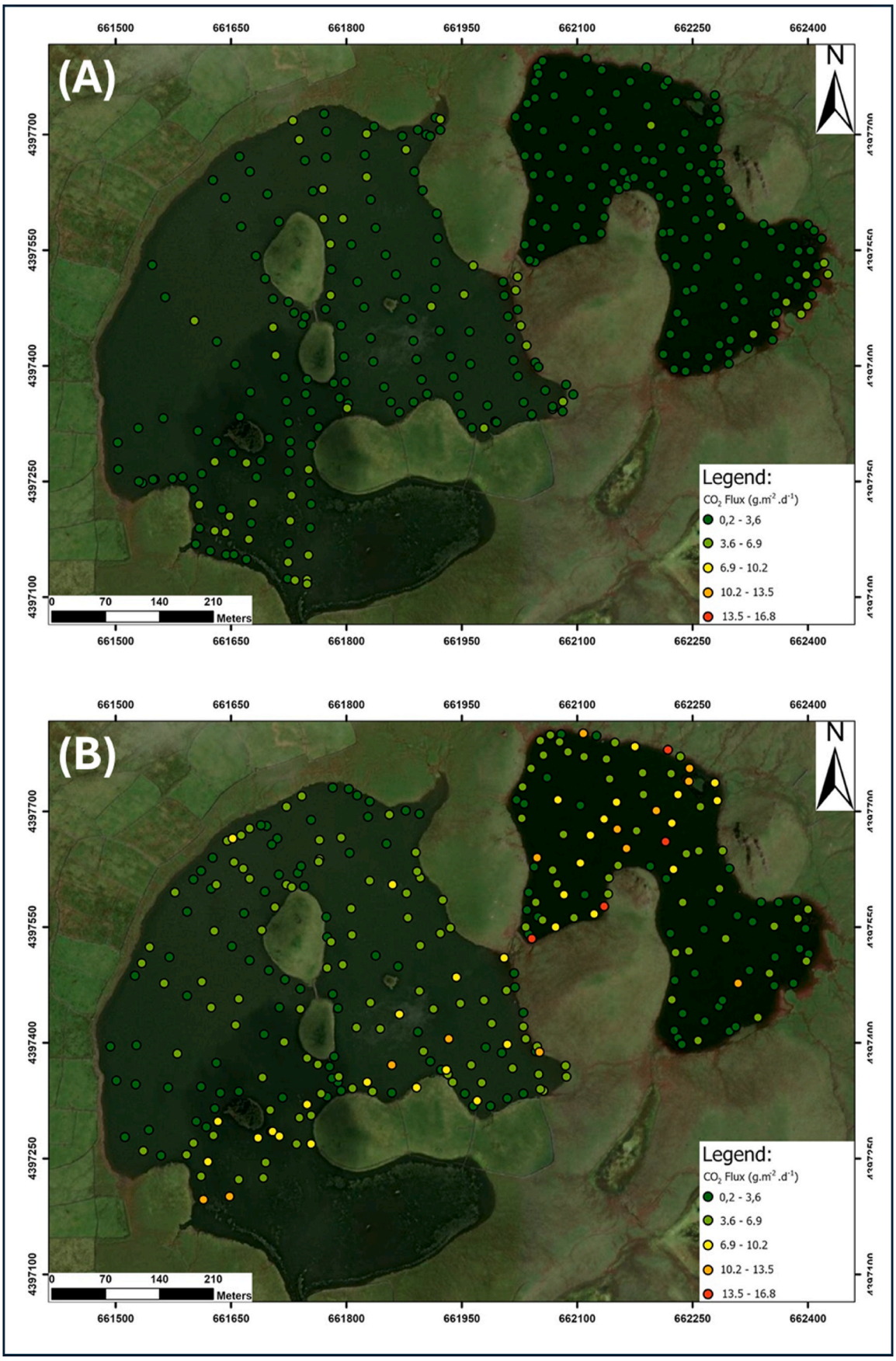

Fig. 3. – ΦCO_2 measurements from surveys conducted in the studied lakes (A, 1st survey; B, 2nd survey).

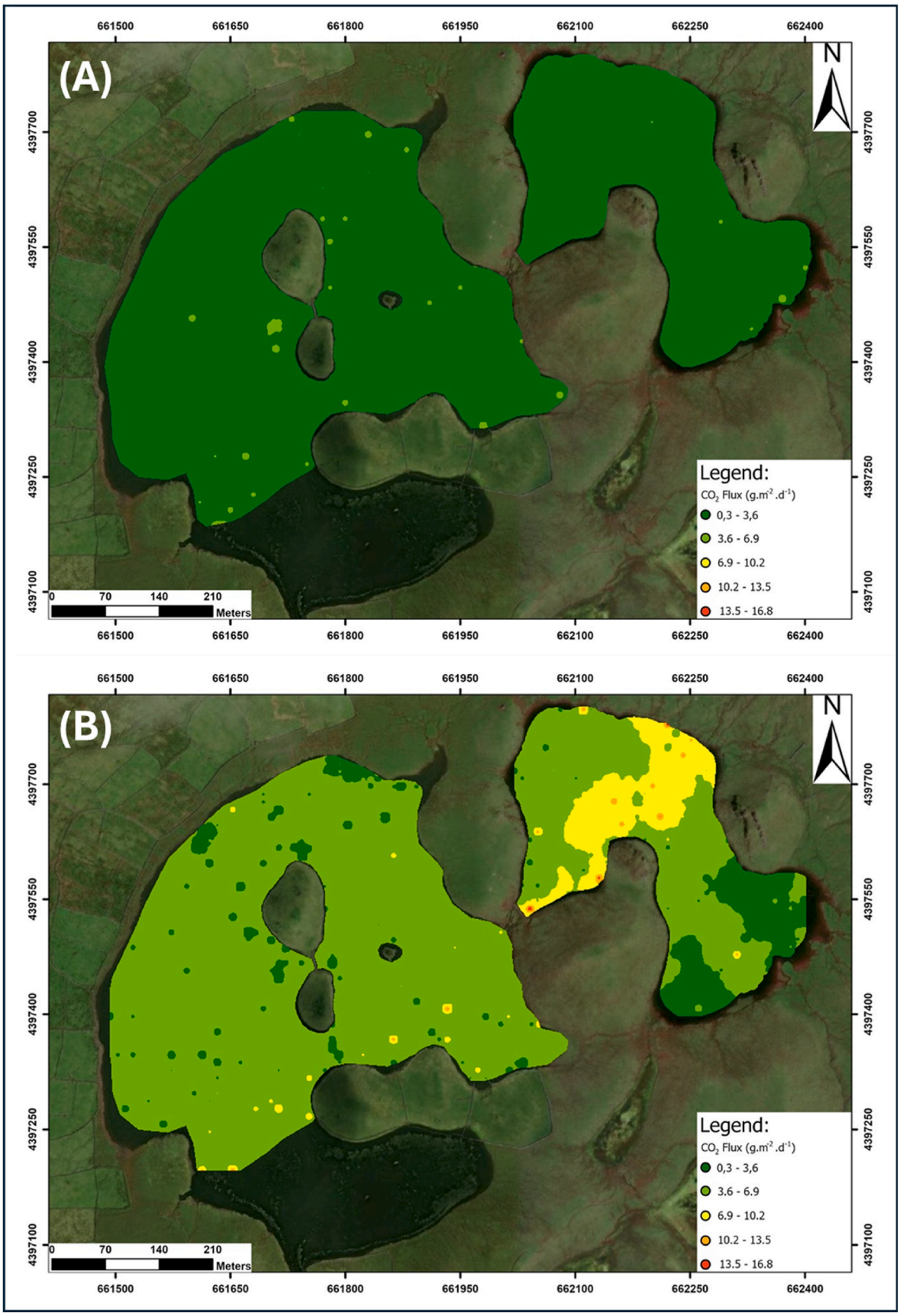

Fig. 4. – E-type ΦCO_2 mapping for Caldeirão Lakes (A, 1st survey; B, 2nd survey).

Table 2
Descriptive statistics of ΦCH_4 in the Caldeirão Lake according to the sampling campaign (n, number of measurements).

Lake	Survey	n	Type	Min. (g m^{-2} d^{-1})	Max. (g m^{-2} d^{-1})	Mean ± SD (g m^{-2} d^{-1})	Median (g m^{-2} d^{-1})
Caldeirão W	3	12	Meas	0.034	0.042	0.038 ± 0.002	0.038
			Calc	0.038	0.048	0.043 ± 0.003	0.044
	4	36	Meas	0.017	0.051	0.031 ± 0.008	0.029
			Calc	0.019	0.045	0.028 ± 0.006	0.027
Caldeirão E	3	12	Meas	0.031	0.039	0.034 ± 0.003	0.035
			Calc	0.040	0.047	0.043 ± 0.003	0.042
	4	36	Meas	0.008	0.033	0.022 ± 0.007	0.024
			Calc	0.009	0.031	0.021 ± 0.006	0.022

communities in the two lakes and across seasons. Caldeirão E and Caldeirão W lakes formed distinct clusters, suggesting that despite their geographic proximity within the same volcanic crater, their microbial assemblages are shaped by localized environmental factors, potentially linked to differences in nutrient loading, hydrodynamics, and sediment characteristics (Fig. 6). Additionally, summer and winter samples are clustered separately within each lake, reinforcing the seasonal stratification of microbial communities. Pairwise comparisons between microbial communities in Summer and Winter also show significant dissimilarities, as indicated by pseudo-F values ranging from 1.15 to 21.37 and p-values below 0.1 in several cases, consistent with the NMDS clustering.

The heatmap analysis for the relative abundance of the several operational taxonomic unit (OTU) shows that, besides reflecting seasonal shifts in microbial composition, the winter communities were characterized by a higher abundance of anaerobic and sulfate-reducing bacteria, such as *Desulfobacteraceae* and *Desulfovibrionaceae*, suggesting that anoxic conditions prevailed during this period (Fig. 7). In contrast, summer samples showed an enrichment in fermentative bacteria, including *Clostridiaceae* and *Enterobacteriaceae*. Differences between the two lakes are also shown by the greater seasonal fluctuations in microbial composition in Caldeirão W compared to Caldeirão E.

4. Discussion

4.1. CO_2 fluxes

The ΦCO_2 values are relatively homogeneous across the surface of both lakes, despite local variations driven by increased biological activity or sediment-related processes (Fig. 4A–B). Values are higher during the 2nd survey compared to the 1st survey (Fig. 3A–B), which aligns with a slightly higher dissolved CO_2 content observed, being the water temperature in the former ~6 °C to ~8 °C higher comparing to the latter survey. However, it is expected that water temperature enhances photosynthetic activity, with the associated decrease on the CO_2 content (Engel et al., 2019; Liang et al., 2017), thus implying ΦCO_2 reduction. This dynamic can lead to a net uptake of atmospheric CO_2, particularly in. shallow lakes (Balmer and Downing, 2011). However, an opposite ΦCO_2 temporal trend is observed in the Caldeirão lakes, suggesting of alternative processes.

As will be further discussed, the composition of microbial community suggests that microbial fermentation and anaerobic organic matter degradation may contribute toward CO_2 release during summer. The slightly lower pH values observed at Caldeirão E Lake suggests that the decomposition of organic matter rate is higher comparing to Caldeirão W, thus influencing pH through the release of free CO_2, as observed in other studies (Sun et al., 2021). As already pointed out, ΦCO_2 values are below the deep-seated CO_2 source threshold, suggesting that CO_2 is mainly of biogenic origin. The δ^{13}C-DIC values further suggests a predominantly biogenic CO_2 source, as the samples from both the surface and bottom of the lakes shows values between −21.85 ‰ and −23.42 ‰ (mean = −22.54 ± −0.70 ‰), which are more negative relative to the typical mantle CO_2 δ^{13}C range (−3.5 to −6; Cartigny et al., 2001) and to the atmospheric δ^{13}C value (about −8.3 ‰; Clark, 2015).

4.2. CH_4 fluxes

Dissolved CH_4 content can be highly variable both spatially and temporally (Hofmann, 2013) and shifts on lake dynamics over time and space drives where and when CH_4 is produced (Ward et al., 2020), resulting in interannual variations on ΦCH_4 from lakes that are often greater than the median diel variability (Smith and Lewis, 1992; Eugster et al., 2020).

Despite the effect of the limited number of transects in the studied lakes, ΦCH_4 fluxes are higher in the 3rd survey (autumn) relative to the 4th survey (winter) (Fig. S6– supplementary material), which reflets the effect of the seasonal variation on temperature. Higher temperatures, like the ones observed during the 3rd survey relative to the 4th survey, may enhance methane production from lake sediments (Fuchs et al., 2016; Duc et al., 2010). Moreover, the dependence on temperature is shown by the expected ΦCH_4 rising due to global warming, as a projected rise in water temperature by 0.86 °C to 2.60 °C by the end of the century may increase CH_4 production rates by 13 %–40 % (Jansen et al., 2022).

Other internal drivers may also cause ΦCH_4 variability in surface water bodies, such as lake depth, surface area, hydrological regime, water level variations and trophic state, as well as external drivers, such as climate and watershed characteristics (Bastviken et al., 2004; Duc et al., 2010; Sanches et al., 2019; Li et al., 2020; Li et al., 21; Yuan et al., 2021; Zhang et al., 2021; Zhong et al., 2023). However, in the present study no relationship was found between the measured ΦCH_4 and depth ($r = 0.281$ and $r = 0.332$, respectively for Caldeirão W and E lakes during the 4th survey; p-values <0.005). Moreover, no significative relationship was also observed between ΦCH_4 and EC ($r = 0.066$ and $r = -0.300$, respectively for Caldeirão W and E lakes during the 4th survey; p-values <0.005), thus not reflecting any control of ΦCH_4 as a function of water salinity as observed in other studies (Liu et al., 2024).

The composition of the microbial communities at the studied lakes may play a key role in CH_4 cycling. As further discussed, microbial data suggests that during summer methanogenesis is enhanced, although no direct measurements of ΦCH_4 are available to test this hypothesis. Inversely, microbial communities composition suggests that methanotrophy may occur during winter, thus contributing toward CO_2 release through the activity of methanotrophic bacteria (Langenegger et al., 2022), a process that is effective in reducing methane emissions from surface water bodies (Sawakuchi et al., 2016).

The balance between methane oxidation and formation depends on several environmental drivers, such as temperature (Duc et al., 2010) or the hydrological regime of the water body. If oxygen availability favors the conversion of CH_4 in CO_2 (Bastviken et al., 2002), shorter gas transport pathways are expected in shallow lakes (Li et al., 2020), thus reducing methane oxidation. Water table variations over time also influence both MOX and methane formation in wetlands (Ward et al., 2020), and in the Caldeirão lakes, water level data, collected by the local water authorities, points out to annual variations of about ±0.8 m, potentially affecting the CH_4 dynamics.

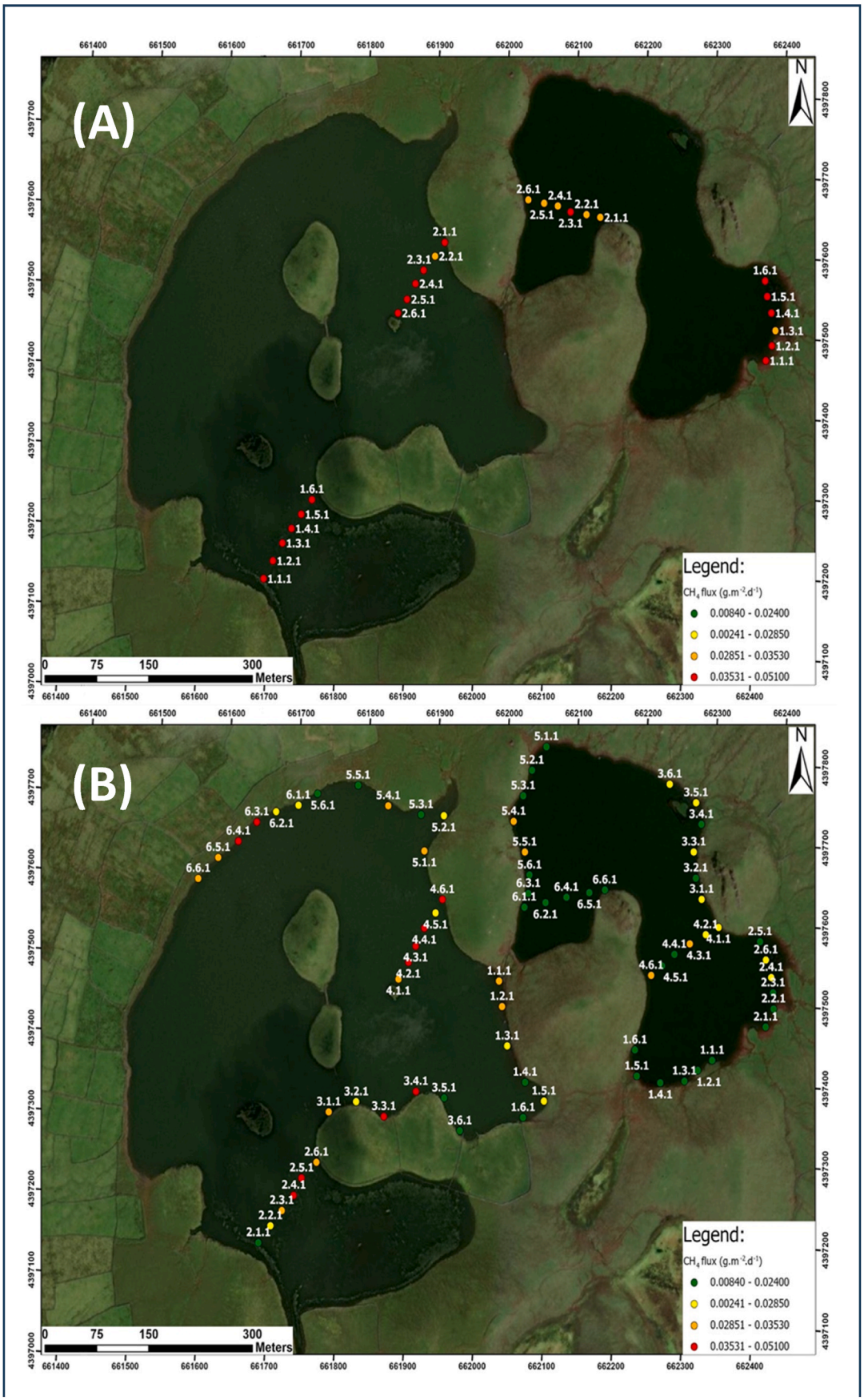

Fig. 5. – ΦCH_4 measurements from different sampling campaigns in the studied lakes (A, 3rd survey; B, 4th survey).

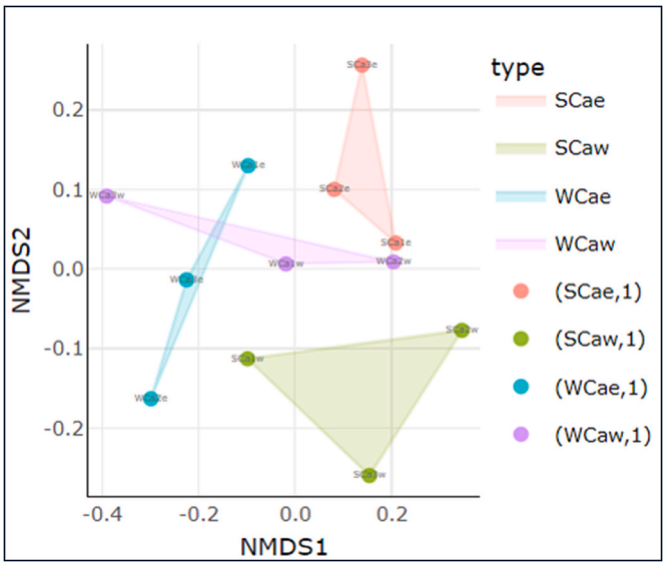

Fig. 6. – Non-metric multidimensional scaling (NMDS) analysis of microbial community composition in sediment samples from Caldeirão E (CaE) and Caldeirão Wt (CaW) during summer (S) and winter (W) (each point represents a replicate sample, and the polygons indicate grouping by season and lakes) The stress value in the NMDS plot is below 0.1.

The hypothesis that the conversion of CH_4 in CO_2 is also influencing both ΦCO_2 and ΦCH_4 is also supported by the evidence of oxygen depletion, as suggested by N_2/O_2 molal ratio data, that exceeds the ASW ratio (~1.9; Ghioldi, 2021), which is particularly noticeable along the 3rd survey, and by the fact that dissolved CO_2 and CH_4 contents depict an inverse linear relationship, although weak ($r = -0.350$; p-value <0.005), mainly during the 3rd survey. Moreover, the close linear relationship between CH_4 content and Ar/O_2 during the same survey suggests that relatively high methane contents are associated with oxygen depletion, further supporting the role of biological activity in regulating both ΦCO_2 and ΦCH_4

4.3. Microbial community and gas fluxes

4.3.1. Microbial activity and ΦCO_2

As shown, microbial communities in Caldeirão lakes depict significant seasonal variations (Table 3), which may control ΦCO_2 and ΦCH_4 through distinct metabolic pathways that regulate greenhouse gas emissions (Table S7 – supplementary material). The observed seasonal changes are consistent with the observed higher CO_2 fluxes in summer, when microbial respiration intensifies.

CO_2 production in the studied lakes results mainly from microbial fermentation and anaerobic organic matter degradation. In winter, sulfate-reducing bacteria (*Desulfobacteraceae* and *Desulfovibrionaceae*) present high OTU counts (Caldeirão E – 210; Caldeirão W - 180), suggesting enhanced sulfate respiration under anoxic conditions. Metal-reducing bacteria, particularly *Geobacteraceae* (OTU: Caldeirão E – 160; Caldeirão W - 140), contribute to CO_2 release through iron reduction. Additionally, *Rhodocyclaceae*, associated with denitrification, show higher abundance in winter, further supporting increased anaerobic respiration.

Warmer temperatures during summer enhance microbial metabolism, leading to increased decomposition rates, and subsequent GHG emissions. In summer, fermentative bacteria become more dominant, particularly *Clostridiaceae* (OTU: Caldeirão E – 315, Caldeirão W - 290) and *Enterobacteriaceae* (OTU: Caldeirão E – 280; Caldeirão W _- 260), reflecting increased organic matter degradation from pasture runoff, which enhances microbial activity and supports greater community heterogeneity. These bacteria facilitate anaerobic fermentation, producing CO_2 alongside intermediary metabolites such as acetate and hydrogen. *Syntrophobacteraceae* remain relatively stable across seasons (OTU: Caldeirão E – ~170; Caldeirão W - ~150), indicating a continuous role in syntrophic degradation processes.

4.3.2. Microbial activity and ΦCH_4

Microbial data suggest that CH_4 production is primarily driven by methanogenic activity during summer, being the presence of methanogenic archaea, such as *Methanobacteriaceae* and *Methanosarcinaceae*. In summer, *Methanobacteriaceae* (OTU: Caldeirão E – 210; Caldeirão W - 195) increase significantly, favoring hydrogenotrophic methanogenesis, while *Methanosarcinaceae* (OTU: Caldeirão E – 180; Caldeirão W - 170) contribute to acetoclastic methanogenesis. The activity of *Smithellaceae* and *Syntrophaceae*, which degrade fatty acids into acetate and hydrogen, is also elevated in summer, promoting CH_4 production. Therefore, although not measured during the 2nd survey, microbial data suggests that CH_4 release may be higher during summer.

Conversely, methane oxidation is more prominent in winter, with *Methylomonadaceae* (OTU: Caldeirão E – 250; Caldeirão W - 230) and *Methylococcaceae* (OTU: Caldeirão E – 210; Caldeirão W - 200) displaying higher abundances. These methanotrophs play a crucial role in CH_4 removal, limiting emissions during colder months.

4.4. Trophic status and GHG emissions

Both Caldeirão lakes are currently eutrophic, with annual mean Carlson TSI-TP values in the range between 62 and 67 from 2017 to 2022 (Malcata et al., 2022). Eutrophication may carry elevated ΦCH_4 (Beaulieu et al., 2019; Zhang et al., 2021, 2024), being shallow lakes more vulnerable because a limited self-cleaning capacity (Havens et al., 2001; Li et al., 2020). Several studies have shown that methanogenesis is two to three times higher in eutrophic lakes relative to oligotrophic or mesotrophic systems (Casper, 1992; Ma et al., 2024; West et al., 2016; Yang et al., 2020; Zhang et al., 2021). The Chl-a content is an indicator of the biological productivity in a lake (DelSontro et al., 2018), and when increasing high ΦCH_4 are to be expected, as CO_2-consumption by phytoplankton and further decay of biomass favors CH_4 release to water (Kumar et al., 2023; Zhang et al., 2024).

At Caldeirão W Lake Chl-a ranged between 4.15 μg L^{-1} and 71.52 μg L^{-1} from 2017 to 2022, being the higher value observed in the summer 2020 (Malcata et al., 2022). Moreover, unpublished monitoring data from the Azores water authorities (Directorate Regional for Climate Action and the Environment) show a similar trend, with values generally increasing in the summer (maximum = 60.80 μg L^{-1}; June 2023) and reducing during colder periods (maximum = 9.48 μg L^{-1}; March 2024). Therefore, the 3rd survey was conducted when Chl-a was higher relative to the 4th survey, thus explaining the higher CH_4 production.

Elevated nutrient inputs, primarily nitrogen and phosphorus from agricultural runoff, stimulate primary production in these lakes, leading to increased organic matter deposition. The organic enrichment fosters the proliferation of heterotrophic microbial communities that decompose organic substrates, resulting in heightened CO_2 emissions through aerobic and anaerobic respiration processes. Climate change can exacerbate nutrients input through runoff, as expected from the expected increase frequency of extreme weather events (Yvon-Durocher et al., 2021).

Studies have demonstrated that eutrophication significantly amplifies carbon emissions in freshwater systems, with urban lakes contributing substantially to the global carbon budget (Wang et al., 2024). Furthermore, increased nutrient availability leads to enhanced microbial decomposition of organic material, intensifying CO_2 emissions (Yang et al., 2023). Nevertheless, as already pointed out, methane oxidation may also contribute toward higher ΦCO_2.

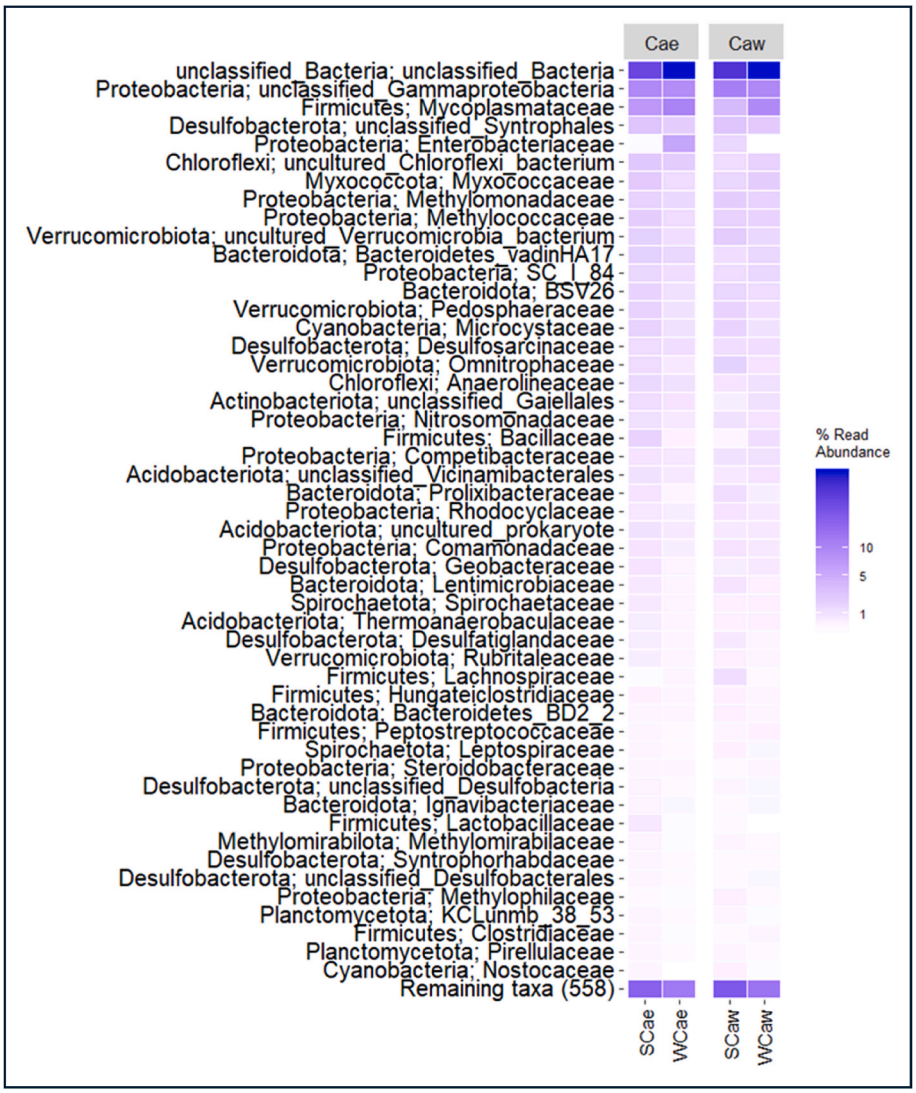

Fig. 7. – Heatmap of OTU relative abundances across sediment samples from Caldeirão East (CaE) and Caldeirão West (CaW) during summer (S) and winter (W). The color gradient represents the relative abundance of OTUs, with warmer colors indicating higher abundance and cooler colors indicating lower abundance.

Table 3
Comparison of the relative abundance (OTUs) of key microbial groups involved in CO_2 and CH_4 cycling in the sediments of Caldeirão E and Caldeirão W lakes during winter and summer.

Microbial Group	Winter OTUs Caldeirão E	Winter OTUs Caldeirão W	Summer OTUs Caldeirão E	Summer OTUs Caldeirão W
CO_2 Producers				
Desulfobacteraceae	210	180	95	85
Desulfovibrionaceae	190	170	100	90
Geobacteraceae	160	140	110	100
Rhodocyclaceae	180	160	130	120
Clostridiaceae	200	185	315	290
Enterobacteriaceae	195	175	280	260
CH_4 Producers				
Methanobacteriaceae	120	110	210	195
Methanosarcinaceae	100	95	180	170
Smithellaceae	90	85	160	150
Syntrophaceae	95	90	175	165
Methane Oxidizers				
Methylomonadaceae	250	230	130	120
Methylococcaceae	210	200	140	130

4.5. Overall GHG emissions

The total CO_2 emission was estimated using the sGs method to be 0.59 t d^{-1} and 0.90 t d^{-1} for the 1st and 2nd surveys at Caldeirão W Lake, respectively, and 0.19 t d^{-1} and 0.43 t d^{-1} at Caldeirão E Lake (Table 4). When integrating the ΦCO_2 values over the lake areas, the fluxes per km^2 were found to be higher at Caldeirão W (3.14 t km^{-2} d^{-1} and 4.66 t km^{-2} d^{-1} for the 1st and 2nd surveys, respectively) compared to Caldeirão E during the 1st survey (2.38 t km^{-2} d^{-1}). However, during the 2nd survey the ΦCO_2 per area was higher at Caldeirão E Lake (6.52 t km^{-2} d^{-1}).

The values obtained from GSA method closely align with those from

Table 4
Overall CO_2 emissions based on GSA and sGs statistical analysis.

Lake	Survey	Working Area (km^2)	ΦCO_2 (t d^{-1}) (sGs)	ΦCO_2 (t d^{-1}) (GSA)	ΦCO_2 (t $km^{-2}d^{-1}$) (sGs)
Caldeirão W	1	0.188	0.59	0.56	3.14
	2	0.193	0.90	0.86	4.66
Caldeirão E	1	0.080	0.19	0.17	2.38
	2	0.066	0.43	0.36	6.52

the sGs approach. GSA estimates for ΦCO_2 ranged from 0.56 t d^{-1} (2.98 t km^{-2} d^{-1}) to 0.86 t d^{-1} (4.46 t km^{-2} d^{-1}) for Caldeirão W, and from 0.17 t d^{-1} (2.13 t km^{-2} d^{-1}) to 0.36 t d^{-1} (5.45 t km^{-2} d^{-1}) for Caldeirão E Lake, corresponding to the 1st and 2nd surveys, respectively (Table 4). These values are generally lower than those found in the ΦCO_2 GSA dataset compiled by Andrade et al. (2024), which includes 45 lake water bodies in the Azores, with fluxes ranging from 0.43 to 508.33 t km^{-2} d^{-1} (mean = 18.05 ± 71.7 t km^{-2} d^{-1}; median = 4.61 t km^{-2} d^{-1}; n = 68). However, when considering only the subset of lakes with depth lower than 5 m the values estimated for Caldeirão W and Caldeirão E lakes fall closer to the mean (5.75 ± 3.26 t km^{-2} d^{-1}) and median (5.0 t km^{-2} d^{-1}; n = 28) of the dataset, mainly in the 2nd survey.

Using as reference the mean CH_4 flux in each water body (Table 2), the overall diffuse CH_4 emission was estimated as 7.14 kg d^{-1} (37.98 kg km^{-2} d^{-1}) and 5.83 kg d^{-1} (31.01 kg km^{-2} d^{-1}), respectively for Caldeirão W Lake during the 3rd and 4th surveys. Considering the spatial heterogeneity of CH_4 concentrations in lakes, and the limited distribution of the transects made in both water bodies, these estimates may have some uncertainty. In both surveys the ΦCH_4 values are in the upper range of the interval proposed by Rosentreter et al. (2021) for lakes with areas between 0.1 and 1 km^2 (Q1 = 6.9 kg km^{-2} d^{-1}; Q3 = 57.0 kg km^{-2} d^{-1}; median = 20.8 kg km^{-2} d^{-1}), being higher that median value. In contrast, Caldeirão E Lake values were respectively equal to 2.52 kg d^{-1} (34.05 kg km^{-2} d^{-1}) and 1.63 kg d^{-1} (22.03 kg km^{-2} d^{-1}) during the two successive surveys, being in the lower range of the dataset bring forward by Rosentreter et al. (2021) for lakes with areas ranging from 0.01 to 0.1 km^2 (Q1 = 12.2 kg km^{-2} d^{-1}; Q3 = 94.4 kg km^{-2} d^{-1}; median = 40.7 kg km^{-2} d^{-1}), but closer to the median along the 3rd survey.

Despite highly temporal and spatial variable, ebullition is often the main pathway for methane flux from surface water bodies (Rosentreter et al., 2021), and high CH_4 emissions have been identified in lakes (Wang et al., 2021, 1021b; Sø et al., 2023). As accounted in global data sets, ebullition may account for 56 %–80 % of CH4 emissions from freshwater lakes (Bauer et al., 2024), and the low reduced water hydrostatic pressure in shallow lakes. Like the ones from Caldeirão, favors bubbles release from sediments DelSontro et al. (2011). Therefore, the actual CH_4 emissions estimated for Caldeirão lakes may be underestimated.

While the ΦCH_4 are lower than those of ΦCO_2, methane is a potent greenhouse gas, with a global warming potential 27 times greater than carbon dioxide over a 100-year period (Forster et al., 2021). Therefore, the total GHG emission (CO_2 plus CH_4) from the studied lakes was estimated to be equal to 1.1 t $CO_{2\text{-eq}}$ d^{-1} and 0.66 t $CO_{2\text{-eq}}$ d^{-1} for Caldeirão W and E, respectively, under warm conditions (2nd and 3rd surveys). During colder conditions (1st and 4th surveys), the GHG emissions ranged from 0.24 t $CO_{2\text{-eq}}$ d^{-1} (Caldeirão E) and 0.59 t $CO_{2\text{-eq}}$ d^{-1} (Caldeirão W), thus about half of values computed for warmer conditions.

Mitigating the environmental impacts on Caldeirão E and Caldeirão W lakes requires comprehensive management strategies aimed at reducing nutrient inputs. Implementing environmental-friendly agricultural practices to minimize runoff, restoring riparian buffer zones, and controlling point-source pollution are essential steps. By addressing the root causes of eutrophication, it is possible to modulate microbial activity and, consequently, GHG emissions, thereby preserving the ecological integrity of these freshwater systems (Schindler et al., 2016).

5. Conclusions

Carbon dioxide and methane fluxes from Caldeirão lakes range from 2.5 t km^{-2} d^{-1} and 6.5 t km^{-2} d^{-1} and from 31 to 38 kg km^{-2} d^{-1}, respectively. Values show a seasonal influence, to which also the shifts in the microbial communities between the winter and summer conditions are associated.

During winter, anaerobic and sulfate-reducing bacteria, such as *Desulfobacteraceae* and *Desulfovibrionaceae*, are abundant, reflecting the prevailing anoxic conditions in colder conditions, during which anaerobic organic matter degradation occurs releasing carbon dioxide. In contrast, fermentative bacteria, such as *Clostridiaceae* and *Enterobacteriaceae*, are enriched in warmer conditions and are known to thrive in environments with high organic matter availability. Microbial fermentation may reflect increased organic matter degradation, resulting from increased runoff from surrounding pastures, which is consistent with the higher chl-a content observed during summer on Caldeirão lakes.

Regarding methane, higher CH_4 production during summer, although not directly measured along the present study during this season, is expected to result from increased methanogenic activity, associated to the presence of methanogenic archaea, such as *Methanobacteriaceae* and *Methanosarcinaceae*. Instead, methane oxidation is more relevant in winter, showing higher abundances of methanotrophs, such as *Methylomonadaceae* and *Methylococcaceae*.

As shown, the high organic matter availability observed mainly during summer is reflected in the microbial activity, that influences ΦCO_2 and ΦCH_4 from the lakes surface into the atmosphere. Mitigating the environmental impacts on Caldeirão E and Caldeirão W lakes requires comprehensive management strategies aimed at reducing nutrient inputs. Implementing environmental-friendly agricultural practices to minimize runoff, restoring riparian buffer zones, and controlling non-point pollution are essential steps. By addressing the root causes of eutrophication, it is possible to modulate microbial activity and, consequently, GHG emissions, thereby preserving the ecological integrity of these freshwater systems (Schindler et al., 2016).

Building on the present study, a broader investigation will be developed to overcome some gaps in the present study namely, to increase representativeness of ΦCH_4 measurements by conducting specific surveys along summer, as well as a denser measurement network, that do to logistical constrains were no possible previously. Moreover, ebullition, although not addressed in the present study, should be fully characterized as this mechanism may be a major pathway for CH_4 release in swallow lakes.

CRediT authorship contribution statement

J. Virgílio Cruz: Writing – review & editing, Writing – original draft, Supervision, Methodology, Investigation, Funding acquisition, Conceptualization. **César Andrade:** Writing – review & editing, Writing – original draft, Methodology, Investigation, Funding acquisition, Conceptualization. **Duarte Toubarro:** Writing – original draft, Methodology, Investigation. **Letícia Ferreira:** Visualization, Investigation. **Adriano Pimentel:** Writing – original draft, Methodology, Investigation. **Fátima Viveiros:** Writing – review & editing, Methodology, Investigation, Conceptualization. **Franco Tassi:** Writing – review & editing, Writing – original draft, Methodology, Investigation. **António Cordeiro:** Investigation. **Diogo Braga:** Visualization, Investigation. **Pedro Raposeiro:** Writing – review & editing, Investigation.

Declaration of competing interest

The authors declare that they have no known competing financial interests or personal relationships that could have appeared to influence the work reported in this paper.

Acknowledgments

This work was supported by FCT – Fundação para a Ciência e Tecnologia, I.P. by project reference 2022.02459.PTDC and DOI identifier 10.54499/2022.02459.PTDC (https://doi.org/10.54499/2022.02459.PTDC).

Letícia Ferreira is supported by a PhD Grant from Fundação para a Ciência e Tecnologia, I.P. (UI/BD/151032/2021). Adriano Pimentel is supported by a CEEC Institutional contract funded by FCT – Fundação

para a Ciência e Tecnologia, I.P. (https://doi.org/10.54499/CEECINST/00024/2021/CP2780/CT0003).

Authors are grateful for the support from two anonymous reviewers that provided detailed comments on preliminary versions of the paper.

Appendix A. Supplementary data

Supplementary data to this article can be found online at https://doi.org/10.1016/j.apgeochem.2025.106529.

Data availability

Data will be made available on request.

References

Andrade, C., Viveiros, F., Cruz, J.V., Coutinho, R., Silva, C., 2016. Estimation of the CO_2 flux from furnas volcanic lake (São Miguel, Azores). J. Volcanol. Geoth. Res. 315, 51–64.

Andrade, C., Viveiros, F., Cruz, J.V., Branco, R., Moreno, L., Silva, C., Coutinho, R., Pacheco, J., 2019a. Diffuse CO_2 flux emission in two maar crater lakes from São Miguel (Azores, Portugal). J. Volcanol. Geoth. Res. 369, 188–202.

Andrade, C., Cruz, J.V., Viveiros, F., Coutinho, R., 2019b. CO_2 flux from volcanic lakes in the western group of the Azores archipelago (Portugal). Water 11, 599.

Andrade, C., Cruz, J.V., Viveiros, F., Branco, R., Coutinho, R., 2019c. CO_2 degassing from Pico Island (Azores, Portugal) volcanic lakes. Limnologica 76, 72–81.

Andrade, C., Viveiros, F., Cruz, J.V., Coutinho, R., Branco, R., 2019d. CO_2 flux from two lakes in volcanic caves in the Azores (Portugal). Appl. Geochem. 102, 218–228.

Andrade, C., Cruz, J.V., Viveiros, F., Coutinho, R., 2020a. CO_2 emissions from Fogo intracaldeira volcanic lakes (São Miguel Island, Azores): a tool for volcanic monitoring. J. Volcanol. Geoth. Res. 400, 106915.

Andrade, C., Cruz, J.V., Viveiros, F., Coutinho, R., 2020b. Diffuse CO_2 emissions from Sete Cidades volcanic lake (São Miguel Island, Azores): influence of eutrophication processes. Environ. Pollut. 268, 115624.

Andrade, C., Viveiros, F., Cruz, J.V., Coutinho, R., 2021. Global carbon dioxide output of volcanic lakes in the Azores archipelago, Portugal. J. Geochem. Explor. 229, 106835. https://doi.org/10.1016/j.gexplo.2021.106835.

Andrade, C., Cruz, J.V., Viveiros, F., Moreno, L., Ferreira, L., Coutinho, R., 2024. Hydrogeochemical evolution and characterization study in volcanic lakes of the Azores archipelago (Portugal). Appl. Geochem. 164, 105933. https://doi.org/10.1016/j.apgeochem.2024.105933.

APHA-AWWA-WPCF, 1985. Standard Methods for the Examination of Water and Methods for the Examination of Water and Wastewater. American Public Health Association, Washington.

Balmer, M., Downing, J., 2011. Carbon dioxide concentrations in eutrophic lakes: undersaturation implies atmospheric uptake. Inland Waters 1, 125–132.

Bastviken, D., Ejlertsson, J., Tranvik, L., 2002. Measurement of methane oxidation in lakes: a comparison of methods. Environ. Sci. Technol. 36, 3354–3361.

Bastviken, D., Cole, J., Pace, M., Tranvik, L., 2004. Methane emissions from lakes: dependence of lake characteristics,two regional assessments, and a global estimate. Glob. Biogeochem. Cycles 18, GB4009. https://doi.org/10.1029/2004GB002238.

Bastviken, D., Tranvik, L.J., Downing, J.A., Crill, P.M., Enrich-Prast, A., 2011. Freshwater methane emissions offset the continental carbon sink. Science 331, 50, 0.1126/science.1196808.

Bauer, P.A., Pinilla, D.H., Glatzel, S., 2024. Is ebullition or diffusion more important as methane emission pathway in a shallow subsaline lake? Sci. Total Environ. 912, 169112. https://doi.org/10.1016/j.scitotenv.2023.169112.

Beaulieu, J.J., DelSontro, T., Downing, J.A., 2019. Eutrophication will increase methane emissionsfrom lakes and impoundments during the 21st century. Nat. Commun. 10, 1375. https://doi.org/10.1038/s41467-019-09100-5.

Bhushana, A., Goyal, V.C., Srivastav, A.L., 2024. Greenhouse gas emissions from inland water bodies and their rejuvenation: a review. J. Water Clim. Change 15, 5626. https://doi.org/10.2166/wcc.2024.561.

Cardellini, C., Chiodini, G., Frondini, F., 2003. Application of stochastic simulation to CO_2 flux from soil. Mapping and quantification of gas release. J. Geophys. Res. 108 (B9), 2425. https://doi.org/10.1029/2002JB002165.

Cartigny, P., Harris, J.W., Javoy, M., 2001. Diamond genesis, mantle fractionations and mantle nitrogen content: a study of $\delta^{13}C$–N concentrations in diamonds. Earth Planet Sci. Lett. 185, 85–98.

Casper, P., 1992. Methane production in lakes of different trophic state. Arch. Hydrobiol. 37, 139–154.

Clark, I., 2015. Groundwater Geochemistry and Isotopes. CRC Press, Taylor & Francis Group, Boca Raton, p. 456.

Chiodini, G., Cioni, R., Guidi, M., Raco, B., Marini, L., 1998. Soil CO_2 flux measurements in volcanic and geothermal areas. Appl. Geochem. 13, 543–552.

Cole, J.J., Caraco, N.F., Kling, G.W., Kratz, T.K., 1994. Carbon dioxide supersaturation in the surface waters of lakes. Science 265, 1568–1570.

Cole, J.J., Bade, D.L., Bastviken, D., Pace, M.L., Van de Bogert, M., 2010. Multiple approaches to estimating air-water gas exchange in small lakes. Limnol Oceanogr. Methods 8, 285–293.

Crusius, J., Wanninnkhof, R., 2003. Gas transfer velocities measured at low wind speed over a lake. Limnol. Oceanogr. 48, 1010–1017.

Cruz, J.V., Antunes, P., França, Z., Nunes, J.C., Amaral, C., 2006. Volcanic lakes from the Azores archipelago (Portugal): geological setting and geochemical characterization. J. Volcanol. Geoth. Res. 156, 135–157.

Cruz, J.V., Pacheco, D., Porteiro, J., Cymbron, R., Mendes, S., Malcata, A., Andrade, C., 2015. Sete Cidades and Furnas lake eutrophication (São Miguel, Azores): analysis of long-term monitoring data and remediation measures. Sci. Total Environ. 520, 168–186.

DelSontro, T., Kunz, M.J., Kempter, T., Wüest, A., Wehrli, B., Senn, D.B., 2011. Spatial heterogeneity of methane ebullition in a large tropical reservoir. Environ. Sci. Technol. 45, 9866–9873.

DelSontro, T., Beaulieu, J.J., Downing, J.A., 2018. Greenhouse gas emissions from lakes and impoundments: upscaling in the face of global change. Limnol. Oceanogr. Lett. 3, 64–75.

Deutsch, C.V., Journel, A.G., 1998. GSLIB: Geostatistical Software Library and User Guide, second ed. Oxford University Press, Oxford, p. 363.

Dias, J., 2001. Geologia e tectónica da ilha do Corvo (Açores - Portugal): Contributos para o ordenamento do espaço físico. University of Coimbra, Coimbra, p. 80 (in Portuguese with English abstract).

DROTRH, 2001. Plano Regional da Água. Relatório técnico. Direção Regional do 990 Ordenamento do Território e do Ordenamento do Território, Ponta Delgada, p. 575 (in Portuguese).

DROTRH, 2021. Plano de Gestão da Região Hidrográfica dos Açores (RH9) 2022-2027 – Relatório Técnico – Versão para consulta pública. Relatório Técnico. Direção Regional do Ordenamento do Território e do Ordenamento do Território, Ponta Delgada 9, 239 (in Portuguese).

Duc, N.T., Crill, P., Bastviken, D., 2010. Implications of temperature and sediment characteristics on methane formation and oxidation in lake sediments. Biogeochemistry 100, 185–196.

Ehhalt, D.H., 1974. The atmospheric cycle of methane. Tellus 26, 58–70.

Engel, F., Drakare, S., Weyhenmeyer, G.A., 2019. Environmental conditions for phytoplankton influenced carbon dynamics in boreal lakes. Aquat. Sci. 81, 35. https://doi.org/10.1007/s00027-019-0631-6.

Eugster, W., DelSontro, T., Shaver, G.R., Kling, G.W., 2020. Interannual, summer, and diel variability of CH_4 and CO_2 effluxes from Toolik Lake, Alaska,during the ice-free periods 2010–2015. Environ. Sci.: Process. Impacts 22, 2181–2198.

Forster, P., Storelvmo, T., Armour, K., Collins, W., Dufresne, J.-L., Frame, D., Lunt, D.J., Mauritsen, T., Palmer, M.D., Watanabe, M., Wild, M., Zhang, H., 2021. The Earth's energy budget, climate feedbacks, and climate sensitivity. In: Masson-Delmotte, V., Zhai, P., Pirani, A., Connors, S.L., Péan, C., Berger, S., Caud, N., Chen, Y., Goldfarb, L., Gomis, M.I., Huang, M., Leitzell, K., Lonnoy, E., Matthews, J.B.R., Maycock, T.K., Waterfield, T., Yelekçi, O., Yu, R., Zhou, B. (Eds.), Climate Change 2021: the Physical Science Basis. Contribution of Working Group I to the Sixth Assessment Report of the Intergovernmental Panel on Climate Change. Cambridge University Press, Cambridge, pp. 923–1054. https://doi.org/10.1017/9781009157896.009.

França, Z., Nunes, J.C., Cruz, J.V., Duarte, H.F., Forjaz, V.H., 2003. Estudo preliminar do vulcanismo da Ilha do Corvo, Açores. In: Garcia, F.G., Valero, J.L. (Eds.), Proceedings da 3ª Assembleia Luso-Espanhola de Geodesia e Geofisica, vol. II. Universidad Politécnica de Valencia, Tomo, pp. 727–730 (in Portuguese with English abstract).

Fuchs, A., Lyautey, E., Montuelle, B., Casper, P., 2016. Effects of increasing temperatures on methane concentrations and methanogenesis during experimental incubation of sedimentsfrom oligotrophic and mesotrophic lakes. J. Geophys. Res. Biogeosci. 121, 1394–1406.

Ghioldi, G.C., 2021. An Appraisal on Methane Emissions from Wetlands Based on Direct Estimates and Theroretical Computations: the Case of Lake Porta Wetland, Northern Tuscany (Italy). Tesi di Laurea Magistrale, Università degli Studi di Firenze, Florence, Italy, p. 92.

Gonçalves, V., 2008. Contribuição para o estudo da qualidade ecológica das lagoas dos açores — fitoplâncton e diatomáceas bentónicas. PhD Thesis Universidade dos Açores, Ponta Delgada 343 (in Portuguese with English abstract).

Guseva, S., Aurela, M., Cortés, A., Kivi, R., Lotsari, E., MacIntyre, S., Mammarella, I., Ojala, A., Stepanenko, V., Uotila, P., Vähä, A., Vesala, T., Wallin, M.B., Lorke, A., 2021. Variable physical drivers of near-surface turbulence in a regulated river. Water Resour. Res. 57, e2020WR027939. https://doi.org/10.1029/2020WR027939.

Havens, K., Fukushima, T., Xie, P., Iwakuma, T., James, R., Takamura, N., Hanazato, T., Yamamoto, T., 2001. Nutrient dynamics and the eutrophication of shallow lakesKasumigaura (Japan), Donghu (PR China), and Okeechobee (USA). Environ. Pollut. 111 (2), 263–272.

Hernández, P.A., Mori, T., Padrón, E., Sumino, H., Pérez, N., 2011. Carbon dioxide emission from Katanuma volcanic lake, Japan. Earth Planets Space 63, 1151–1156.

Hofmann, H., 2013. Spatiotemporal distribution patterns of dissolved methane in lakes: how accurate are the current estimations of the diffusive flux path? Geophys. Res. Lett. 40, 2779–2784.

Holgerson, M., Raymond, P., 2016. Large contribution to inland water CO_2 and CH_4 emissions from very small ponds. Nat. Geosci. 9, 222–226.

IAEA, 2017. Sampling procedures for isotope hydrology. Water Resources Programe 8.

Isaaks, E.H., Srivastava, R.M., 1989. An Introduction to Applied Geostatistics. Oxford University Press, Oxford, p. 561.

Jansen, J., Woolway, R.L., Kraemer, B.M., Albergel, C., Bastviken, D., Weyhenmeyer, G. A., Marcé, R., Sharma, S., Sebastian Sobek, S., Tranvik, L.J., Perroud, M., Golub, M., Moore, T.N., Vinnå, L.R., La Fuente, S., Grant, L., Pierson, D.C., Thiery, W., Jennings, E., 2022. Global increase in methane production under future warming of lake bottom waters. Glob. Change Biol. 28, 5427–5440.

Johnson, M.S., Matthews, E., Du, J., Genovese, V., Bastviken, D., 2022. Methane emission from global lakes: new spatiotemporal data and observation-driven modeling of methane dynamics indicates lower emissions. J. Geophys. Res. Biogeosci. 127, e2022JG006793. https://doi.org/10.1029/2022JG006793.

Kumar, A., Mishra, S., Bakshi, S., Upadhyay, P., Thakur, T.K., 2023. Response of eutrophication and water quality drivers on greenhouse gas emissions in lakes of China: a critical analysis. Ecohydrology 16, 1–10.

Langenegger, T., Vachon, D., Donis, D., McGinnis, D.F., 2022. Methane oxidation dynamics in a stratified lake: insights revealed from a mass balance and carbon stable isotopes. Limnol. Oceanogr. 67, 2157–2173.

Larrea, P., França, Z., Lago, M., Widom, E., Galé, C., Ubide, T., 2013. Magmatic processes and the role of antecrysts in the genesis of Corvo island (Azores archipelago, Portugal). J. Petrol. 54, 769–793.

Lesley, K.S., Lewis, W.M., 1992. Seasonality of methane emissions from five lakes and associated wetlands of the Colorado rockies. Glob. Biogeochem. Cycles 6, 323–338.

Li, L., Fuchs, A., Ortega, S.R., Xue, B., Casper, P., 2021. Spatial methane pattern in a deep freshwater lake: relation to water depth and topography. Sci. Total Environ. 764 (2021), 142829. https://doi.org/10.1016/j.scitotenv.2020.142829.

Li, M., Peng, C., Zhu, Q., Zhou, X., Yang, G., Song, X., Zhang, K., 2020. The significant contribution of lake depth in regulating global lake diffusive methane emissions. Water Res. 172, 115465. https://doi.org/10.1016/J.watres.2020.115465.

Liang, Y.T., Zhang, Y.Y., Wang, N.N., Luo, T.W., Zhang, Y., Rivkin, R.B., 2017. Estimating primary production of picophytoplankton using the carbon-based ocean productivity model: a preliminary study. Front. Microbiol. 8, 1926. https://doi.org/10.3389/fmicb.2017.01926.

Liss, P., Slater, P., 1974. Flux of gases across the air-sea interface. Nature 247, 181–184. https://doi.org/10.1038/247181a0.

Liu, H., Xiao, S., Liu, W., Wang, H., Liu, Z., Li, X., Zhang, P., Liu, J., 2024. Salinity decreases methane concentrations in Chinese lakes. Sci. Total Environ. 937, 173412. https://doi.org/10.1016/j.scitotenv.2024.173412.

Livingston, G.P., Hutchinson, G.L., 1995. Enclosure-based Measurement of Trace Gas Exchange: Applications and Sources of Error. In: Matson, P.A., Harris, R.C. (Eds.), Biogenic Trace Gases: Measuring Emissions from Soil and Water. Blackwell Science, Oxford, pp. 14–51.

Ma, B.J., Wang, Y., Jiang, P., Li, S.Y., 2024. The influence of seasonal variability of eutrophication indicators on carbon dioxide and methane diffusive emissions in the largest shallow urban lake in China. Water-Sui 16, 1–15.

Malcata, A., Pacheco, D., Cymbron, R., 2022. Monitorização da qualidade da água das lagoas de São Miguel, Pico, Flores e Corvo. Comparação de resultados entre 2017 e 2020. SRAAC. Ponta Delgada 336 (in Portuguese).

Martini, M., Giannini, L., Prati, F., Tassi, F., Capaccioni, B., Iozzelli, P., 1994. Chemical characters of crater lakes in the Azores and Italy: the anomaly of Lake Albano. Geochem. J. 28, 173–184.

Martins, G., Ribeiro, D., Pacheco, D., Cruz, J.V., Cunha, R., Gonçalves, V., Nogueira, R., Brito, A.G., 2008. Prospective scenarios for water quality and ecological status in Lake Sete Cidades (Portugal): the integration of mathematical modeling in decision processes. Appl. Geochem. 23, 2171–2181.

Martins, G., Henriques, I., Ribeiro, D.C., Correia, A., Bodelier, P.L.E., Cruz, J.V., Brito, A.G., Nogueira, R., 2012. Bacterial diversity and geochemical profiles in sediments from eutrophic Azorean lakes. Geomicrobiol. J. 29, 704–715.

Mazot, A., Bernard, A., 2015. CO_2 degassing from volcanic. In: Rouwet, D., Christenson, B., Tassi, F., Vandemeulebrouck, J. (Eds.), Volcanic Lakes, Advances in Volcanology. Springer, Heidelberg, pp. 341–354.

Mazot, A., Taran, Y., 2009. CO_2 flux from the volcanic lake of el chichon (Mexico). Geofis. Int. 48, 73–83.

Melo, C.S., Ramalho, R.S., Quartau, R., Hipólito, A., Gil, A., Borges, P.A., Cardigos, F., Ávila, S.P., Madeira, J., Gaspar, J.L., 2018. Genesis and morphological evolution of coastal talus-platforms (fajãs) with lagoons: the case study of the newly-formed Fajã dos Milagres (Corvo Island, Azores). Geomorphology 310, 138–152.

Nisbet, E.G., Manning, M.R., Dlugokencky, E.J., Fisher, R.E., Lowry, D., Michel, S.E., Myhre, C.L., Platt, S.M., Allen, G., Bousquet, P., Brownlow, R., Cain, M., Francel, J.L., Hermansen, O., Hossaini, R., Jones, A.E., Levin, I., Manning, A.C., Myhre, G., Pyle, J.A., Vaughn, B.H., Warwick, N.J., White, J.W.C., 2019. Very strong atmospheric methane growth in the 4 years 2014–2017: implications for the Paris Agreement. Glob. Biogeochem. Cycles 33, 318–342.

Nunes, L.J.R., 2023. The rising threat of atmospheric CO_2: a review on the causes, impacts, and mitigation strategies. Environments 10, 66. https://doi.org/10.3390/environments10040066.

Pacheco, D., Cruz, J.V., Malcata, A., Mendes, S., 2005. Monitorização da qualidade da água das lagoas de São Miguel. SRAM, Ponta Delgada, p. 178 (in Portuguese).

Pacheco, D., Malcata, A., Mendes, S., Cruz, J.V., Gaspar, J.L., 2010. Monitorização da qualidade da água das lagoas de São Miguel. Comparação de resultados entre 2004 e 2008. SRAM, Ponta Delgada, p. 211 (in Portuguese).

Pacheco, J.M., Ferreira, T., Queiroz, G., Wallenstein, N., Coutinho, R., Cruz, J.V., Pimentel, A., Silva, R., Gaspar, J.L., Goulart, C., 2013. Notas sobre a geologia do arquipélago dos Açores. In: Dias, R., Araújo, A., Terrinha, P., Kullberg, J.C. (Eds.), Geologia de Portugal, vol. 2. Escolar Editora, pp. 595–690 (in Portuguese).

Porteiro, J., 2000. Lagoas dos Açores: elementos de suporte ao planeamento integrado. PhD Thesis. Universidade dos Açores, Ponta Delgada (in Portuguese).

Raymond, P.A., Hartmann, J., Lauerwald, R., Sobek, S., McDonald, C., Butman, D., Striegl, R., Mayorga, E., Humborg, C., Kortelainen, P., Durr, H., Meybeck, M., Ciais, P., Guth, P., 2013. Global carbon dioxide emissions from inland waters. Global carbon dioxide emissions from inland waters. Nature 503, 355–359.

Ribeiro, D.C., Martins, G., Nogueira, R., Cruz, J.V., Brito, A.G., 2008. Phosphorus fractionation in volcanic lake sediments (Azores — Portugal). Chemosphere 70, 1256–1263.

Rocher-Ros, G., Stanley, E.H., Loken, L.C., Casson, N.J., Raymond, P.A., Liu, S., Amatulli, G., Sponseller, R.A., 2023. Global methane emissions from rivers and streams. Nature 621, 530–535.

Rosentreter, J.A., Borges, A.V., Deemer, B.R., Holgerson, M.A., Liu, S., Song, C., Melack, J., Raymond, P.A., Duarte, C.M., Allen, G.H., Olefeldt, D., Poulter, B., Battin, T.I., Eyre, B.D., 2021. Half of global methane emissions come from highly variable aquatic ecosystem sources. Nat. Geosci. 14, 225–230.

Sanches, L.F., Guenet, B., Marinho, C.C., Barros, N., Esteves, F.A., 2019. Global regulation of methane emissions from natural lakes. Sci. Rep. 9, 255. https://doi.org/10.1038/s41598-018-36519-5.

Santos, M., Pacheco, D., Santana, A.F., Muelle, H., 2005. Cyanobacteria blooms in sete cidades lake (São Miguel island — Azores). Algol. Stud. 117, 393–406.

Saunois, M., Bousquet, P., Poulter, B., Peregon, A., Ciais, P., Canadell, J.G., Dlugokencky, E.J., Etiope, G., Bastviken, D., Houweling, S., Janssens-Maenhout, G., Tubiello, F.N., Castaldi, S., Jackson, R.B., Alexe, M., Arora, V.K., Beerling, D.J., Bergamaschi, P., Blake, D.R., Brailsford, G., Brovkin, V., Bruhwiler, L., Crevoisier, C., Crill, P., Covey, K., Curry, C., Frankenberg, C., Gedney, N., Höglund-Isaksson, L., Ishizawa, M., Ito, A., Joos, F., Kim, H.-S., Kleinen, T., Krummel, P., Lamarque, J.-F., Langenfelds, R., Locatelli, R., Machida, T., Maksyutov, S., McDonald, K.C., Marshall, J., Melton, J.R., Morino, I., Naik, V., O'Doherty, S., Parmentier, F.-J.W., Patra, P.K., Peng, C., Peng, S., Peters, G.P., Pison, I., Prigent, C., Prinn, R., Ramonet, M., Riley, W.J., Saito, M., Santini, M., Schroeder, R., Simpson, I.J., Spahni, R., Steele, P., Takizawa, A., Thornton, B.F., Tian, H., Tohjima, Y., Viovy, N., Voulgarakis, A., van Weele, M., van der Werf, G.R., Weiss, R., Wiedinmyer, C., Wilton, D.J., Wiltshire, A., Worthy, D., Wunch, D., Xu, X., Yoshida, Y., Zhang, B., Zhang, Z., Zhu, Q., 2016. The global methane budget 2000-2012. Earth Syst. Sci. Data 8, 697–751. https://doi.org/10.5194/essd-8-697-2016.

Saunois, M., Stavert, A.R., Poulter, B., Bousquet, P., Canadell, J.G., Jackson, R.B., Raymond, P.A., Dlugokencky, E.J., Houweling, S., Patra, P.K., Ciais, P., Arora, V.K., Bastviken, D., Bergamaschi, P., Blake, D.R., Brailsford, G., Bruhwiler, L., Carlson, K.M., Carrol, M., Castaldi, S., Chandra, N., Crevoisier, C., Crill, P.M., Covey, K., Curry, C.L., Etiope, G., Frankenberg, C., Gedney, N., Hegglin, M.I., Höglund-Isaksson, L., Hugelius, G., Ishizawa, M., Ito, A., Janssens-Maenhout, G., Jensen, K.M., Joos, F., Kleinen, T., Krummel, P.B., Langenfelds, R.L., Laruelle, G.G., Liu, L., Machida, T., Maksyuto, S., McDonald, K.C., McNorton, J., Miller, P.A., Melton, J.R., Morino, I., Müller, J., Murguia-Flores, f., Naik, V., Niwa, Y., Noce, S., O'Doherty, S., Parker, R.J., Peng, C., Peng, S., Peters, G.P., Prigent, C., Prinn, R., Ramonet, M., Regnier, M., Riley, W.J., Rosentreter, J.A., Segers, A., Simpson, I.J., Shi, H., Smith, S.J., Steele, L.P., Thornton, B.F., Tian, H., Tohjima, Y., Tubiello, F.N., Tsuruta, A., Viovy, N., Voulgarakis, A., Weber, T.S., van Weele, M., van der Werf, G.R., Weiss, R.F., Worthy, D., Wunch, D., Yin, Y., Yoshida, Y., Zhang, W., Zhang, Z., Zhao, Y., Zheng, B., Zhu, Q., Zhu, Q., Zhuang, Q., 2020. The global methane budget 2000–2017. Earth Syst. Sci. Data 12, 1561–1623.

Sawakuchi, H.O., Bastviken, D., Sawakuchi, A.O., Ward, N.D., Borges, C.D., Tsai, S.M., Richey, J.E., Ballester, M.V.R., Krusche, A.V., 2016. Oxidative mitigation of aquatic methane emissions in large Amazonian rivers. Glob. Change Biol. 22, 1075–1085.

Sáez, A., Hernández, A., Pimentel, A., Andrade, M., Bao, R., Raposeiro, P.M., Gonçalves, V., Benavente, M., Pla-Rabes, S., Ramalho, R., Giralt, S., 2025. Westerlies migrations and volcanic records over the past 4000 years from the Azores lacustrine sequences. Exploring correlations and impacts on Western Europe. Global Planet. Change 246, 104698. https://doi.org/10.1016/j.gloplacha.2025.104698.

Schindler, D.W., Hecky, R.E., McCullough, G.K., 2016. The rapid eutrophication of freshwater ecosystems: causes, consequences, and future implications. Science 331, 1448–1450.

Sinclair, A.J., 1974. Selection of threshold values in geochemical data using probability graphs. J. Geochem. Explor. 3, 129–149.

Smith, L.K., Lewis, W.M., 1992. Seasonality of methane emissions from five lakes and associated wetlands of the Colorado rockies. Glob. Biogeochem. Cycles 6, 323–338.

Sø, J.S., Sand-Jensen, K., Martinsen, K.T., Polauke, E., Kjær, J.E., Reitzel, K., Kragh, T., 2023. Methane and carbon dioxide fluxes at high spatiotemporal resolution from a small temperate lake. Sci. Total Environ. 878, 162895. https://doi.org/10.1016/j.scitotenv.2023.162895.

St Louis, V.L., Kelly, C.A., Duchemin, É., Rudd, J.W., Rosenberg, D.M., 2000. Reservoir surfaces as sources of greenhouse gases to the atmosphere: a global estimate. Bioscience 50, 766–775.

Stackebrandt, E., Goodfellow, M., 1991. Nucleic acid techniques in bacterial systematics. In: Stackebrandt, E., Goodfellow, M. (Eds.), 16S rRNA Sequencing Primers. Wiley, New York, pp. 132–136.

Sun, H., Lu, X., Yu, R., Yang, J., Liu, X., Cao, Z., Zhang, Z., Li, M., Geng, Y., 2021. Eutrophication decreased CO_2 but increased CH_4 emissions from lake: a case study of a shallow Lake. Water Res. 201, 117363. https://doi.org/10.1016/j.watres.2021.117363.

Tassi, F., Nisi, B., Cardellini, C., Capecchiacci, F., Donnini, M., Vaselli, O., Avino, R., Chiodini, G., 2013. Diffuse soil emission of hydrothermal gases (CO_2, CH_4, and C_6H_6) at Solfatara crater (Campi Flegrei, southern Italy). Appl. Geochem. 35, 142–153.

Tassi, F., Cabassi, J., Andrade, C., Callieri, C., Silva, C., Viveiros, F., Corno, G., Vaselli, O., Selmo, E., Gallorini, A., Ricci, A., Giannini, L., Cruz, J.V., 2018. Mechanisms regulating CO_2 and CH_4 dynamics in the Azorean volcanic lakes (São Miguel Island, Portugal). J. Limnol. 77 (3), 483–504.

Tranvik, L.J., Downing, J.A., Cotner, J.B., Loiselle, S.A., Striegl, R.G., Ballatore, T.J., Dilon, P., Finlay, K., Fortino, K., Knoll, L.B., Kortelainen, P.L., Kutser, T., Larsen, S., Laurion, I., Leech, D.M., McCallister, S.L., McKnight, D.M., Melack, J.M., Overholt, E., Porter, J.A., Prairie, Y., Renwick, W.H., Roland, F., Sherman, B.S., Schindler, D.W., Sobek, S., Tremblay, A., Vanni, M.J., Verschoor, A.M., Von Wachenfeldt, E., Weyhenmeyer, G.A., 2009. Lakes and reservoirs as regulators of carbon cycling and climate. Limnol. Oceanogr. 54, 2298–2314.

Viveiros, F., Cardellini, C., Ferreira, T., Caliro, S., Chiodini, G., Silva, C., 2010. Soil CO_2 emissions at Furnas Volcano, São Miguel Island, Azores archipelago: volcano monitoring perspectives, geomorphologic studies, and land use planning application. J. Geophys. Res. 115, B12208, 1-17.

Venturi, S., Tassi, F., Cabassi, J., Randazzo, A., Lazzaroni, M., Capecchiacci, F., Vietina, B., Vaselli, O., 2021. Exploring methane emission drivers in wetlands: the cases of Massaciuccoli and Porta Lakes (Northern Tuscany, Italy). Appl. Sci. 11, 12156. https://doi.org/10.3390/app112412156.

Walter, B., Heimann, M., Matthews, E., et al., 2001. Modeling modern methane emissions from natural wetlands 1. Model description and result. J. Geophys. Res. 106, 34189–34206.

Wang, G., Xia, X., Liu, S., Zhang, L., Zhang, S., Wang, J., Xi, N., Zhang, Q., 2021. Intense methane ebullition from urban inland waters and its significant contribution to greenhouse gas emissions. Water Res. 189, 116654. https://doi.org/10.1016/j.watres.2020.116654.

Wang, H., Lu, Y., Li, Y., Zhang, Q., 2024. Urban lakes and their role in carbon cycling: an underestimated component of the global carbon budget. Environ. Sci. Technol. 58 (3), 1256–1269. https://doi.org/10.1021/acs.est.3c06532.

Wanninnkhof, R., 2014. Relationship between wind speed and gas exchange over the ocean revisited. Limnol Oceanogr. Methods 12, 351–362.

Ward, N., Bianchi, T.S., Martin, J.B., Quintero, C.J., Sawakuchi, H.O., Cohen, M.J., 2020. Pathways for methane emissions and oxidation that influence the net carbon balance of a subtropical cypress swamp. Front. Earth Sci. 8, 573357. https://doi.org/10.3389/feart.2020.573357.

West, W.E., Creamer, K.P., Jones, S.E., 2016. Productivity and depth regulate lake contributions to atmospheric methane. Limnol. Oceanogr. 61, s51–s61.

Wuebles, D.J., Hayhoe, K., 2002. Atmospheric methane and global change. Earth Sci. Rev. 57, 177–210.

Yang, Y., Chen, J., Tong, T., Xie, S., Liu, Y., 2020. Influences of eutrophication on methanogenesis pathways and methanogenic microbial community structures in freshwater lakes. Environ. Pollut. 260, 114106. https://doi.org/10.1016/j.envpol.2020.114106.

Yuan, X., Liu, Q., Cui, B., Xu, X., Liang, L., Sun, T., Yan, S., Wanga, X., Li, C., Li, S., Li, M., 2021. Effect of water-level fluctuations on methane and carbon dioxide dynamics in a shallow lake of Northern China: implications for wetland restoration. J. Hydrol. 597, 126169. https://doi.org/10.1016/j.jhydrol.2021.126169.

Yang, X., Liu, Z., Xu, X., Zhang, B., 2023. Microbial decomposition of organic matter and its contribution to CO_2 fluxes in eutrophic lakes. Limnol. Oceanogr. 68 (2), 378–391. https://doi.org/10.1002/lno.12345.

Yvon-Durocher, G., Allen, A.P., Bastviken, D., Conrad, R., Gudasz, C., St-Pierre, A., del Giorgio, P.A., 2021. Methane fluxes show consistent temperature dependence across microbial to ecosystem scales. Nature 535, 193–197.

Zhang, L., Liao, Q., Gao, R., Luo, R., Liua, C., Zhonga, J., Wanga, Z., 2021. Spatial variations in diffusive methane fluxes and the role of eutrophication in a subtropical shallow lake. Sci. Total Environ. 759, 143495. https://doi.org/10.1016/j.scitotenv.2020.143495.

Zhang, J., Cao, L., Liu, Z., Wan, L., Cao, X., Zhou, Y., Songa, C., 2024. Relationship between eutrophication and greenhouse gases emission in shallow freshwater lakes. Sci. Total Environ. 925, 171610. https://doi.org/10.1016/j.scitotenv.2024.171610.

Zhong, J., Yang, F., Zhang, M., Sun, C., Wang, S., Chen, Q., Wanga, H., Zhang, L., 2023. Water depth and productivity regulate methane (CH_4) emissions from temperate cascade reservoirs in northern China. J. Hydrol. 626, 130170. https://doi.org/10.1016/j.jhydrol.2023.130170.

Zhu, Q., Peng, C., Chen, H., Fang, X., Liu, J., Jiang, H., Yang, Y., Yang, G., 2015. Estimating global natural wetland methane emissions using process modelling: spatio-temporal patterns and contributions to atmospheric methane fluctuations. Global Ecol. Biogeogr. 24, 959–972.